Geochimica et Cosmochimica Acta 342 (2023) 156–168

Contents lists available at ScienceDirect

Geochimica et Cosmochimica Acta

journal homepage: www.elsevier.com/locate/gca

Chondrite diversity revealed by chromium, calcium and magnesium isotopes

Ke Zhu ("朱柯") [a,b,*], Martin Schiller [c], Frédéric Moynier [b], Mirek Groen [c], Conel M.O'D. Alexander [d], Jemma Davidson [e], Devin L. Schrader [e], Addi Bischoff [f], Martin Bizzarro [c]

[a] Freie Universität Berlin, Institut für Geologische Wissenschaften, Malteserstr. 74-100, 12249 Berlin, Germany
[b] Université Paris Cité, Institut de Physique du Globe de Paris, CNRS UMR 7154, 1 rue Jussieu, Paris 75005, France
[c] Centre for Star and Planet Formation, Globe Institute, University of Copenhagen, Øster Voldgade 5–7, Copenhagen DK-1350, Denmark
[d] Earth and Planets Laboratory, Carnegie Institution for Science, 5241 Broad Branch Road, Washington, DC 20015, USA
[e] Buseck Center for Meteorite Studies, School of Earth and Space Exploration, Arizona State University, 781 East Terrace Road, Tempe, AZ 85287-6004, USA
[f] Institut für Planetologie, Westfälische Wilhelms-Universität Münster, Wilhelm-Klemm-Str. 10, 48149 Münster, Germany

ARTICLE INFO

Article history:
Received 9 April 2022
Accepted 9 December 2022
Available online 13 December 2022
Associate editor: Stefan Weyer

Keywords:
Chondrites
Cr, Ca and Mg isotopes
Mass-independent isotope fractionation
CC-NC dichotomy
^{26}Al-^{26}Mg Isochron
^{53}Mn-^{53}Cr Isochron
Meteorite classification

ABSTRACT

Chondrites are undifferentiated meteorites that can provide information on the compositions of materials in the early solar System, including the building blocks of the terrestrial planets. While most chondrites belong to well-defined groups based on their mineralogy and chemical composition, a minor fraction have unusual characteristics and are classified as ungrouped chondrites. These ungrouped chondrites reflect the diversity of chondritic materials in the early solar system; however, they are not as well studied as grouped meteorites and their origins are poorly understood. In this study, we present high-precision mass-independent Cr, Ca and Mg isotope data for 17 ungrouped chondrites. The ε^{54}Cr and ε^{48}Ca (ε expresses parts per ten thousand mass-independent isotope deviation) data for ungrouped chondrites also provide important constraints for assessing their relationships to the known chondrite groups, and the radiogenic Mg isotope ratios (μ^{26}Mg*) can be used to track the early solar system history. We also present the first high-precision data for a Kakangari (KC) chondrite, an enstatite chondrite, and for four enstatite-rich meteorites. The ε^{54}Cr and ε^{48}Ca values for the KC are -0.44 ± 0.04 and -1.30 ± 0.25, respectively, and ε^{48}Ca value for SAH 97096 (EH3) is -0.19 ± 0.22 that overlaps with that of those of Earth-Moon system and ordinary chondrites. All the carbonaceous chondrite-like (CC) ungrouped chondrites show positive ε^{54}Cr and ε^{48}Ca values, and all the non-carbonaceous chondrite-like (NC) ungrouped chondrites and KCs (also belong to the NC trend) show zero or negative ε^{54}Cr and ε^{48}Ca values. This observation confirms the CC-NC dichotomy for primitive solar system materials. LEW 87232 (KC) also shows the highest ^{55}Mn/^{52}Cr ratio and ε^{53}Cr value amongst all the chondrites. There is a positive trend between ^{55}Mn/^{52}Cr ratios and ε^{53}Cr values among all the chondrites that mostly reflects a mixing between multiple chondritic components. Previously it has been reported that there is a bulk ^{26}Al-^{26}Mg correlation line amongst chondrites. This correlation has been interpreted as being due to mixing of CAIs (high ^{27}Al/^{24}Mg ratios and μ^{26}Mg* values) and other silicate material (e.g., chondrules and matrix). By providing additional ^{26}Al-^{26}Mg chondrite data, we show that there is no ^{26}Al-^{26}Mg correlation line for the chondrites, ruling out the two-endmember (i.e., CAIs and other silicates) mixing model.

1. Introduction

Chondrites are the oldest cosmic sedimentary rocks, the most pristine of which preserve information about the origin and early evolution of the Solar System (e.g., Krot et al., 2014). Most of the parent bodies of chondrites did not undergo significant melting (though most underwent varying degrees of thermal metamorphism) and thus did not differentiate. Therefore, bulk chondrite samples have chemical compositions that are thought to be representative of their bulk parent bodies and have been taken as proxies for the compositions of bulk differentiated planets such as the Earth (Allègre et al., 1995). Chondrites represent the best suited samples to investigate the evolution of the Solar System and planet formation.

* Corresponding author at: Bristol Isotope Group, School of Earth Sciences, University of Bristol, Wills Memorial Building, Queen's Road, Bristol BS8 1RJ, United Kingdom.
E-mail address: ke.zhu@bristol.ac.uk (K. Zhu).

https://doi.org/10.1016/j.gca.2022.12.014
0016-7037/

Most chondrites have been classified into distinct groups (e.g., Krot et al., 2014) based on similarities in petrological, chemical and isotopic characteristics. Each of these groups potentially represent a distinct parent body. However, there are a minority of chondrites that are ungrouped (e.g., Bischoff et al., 2021; Torrano et al., 2021; Zolensky et al., 2002) that represent a diversity of poorly sampled chondrite parent bodies.

The chondrite groups also exhibit large chemical and isotopic variations (Alexander, 2019a, b; Kleine et al., 2020; Palme and O'Neill, 2014; Warren, 2011) that are the result of nebular and parent body accretion processes. The variations in nucleosynthetic isotopic anomalies in Cr, Ti, and Ca between different groups of chondrites, reported as ε^{54}Cr (Shukolyukov and Lugmair, 2006; Trinquier et al., 2007), ε^{50}Ti (Leya et al., 2008) and ε^{48}Ca (Chen et al., 2011), have been shown to be robust tracers of genetic relationships between chondrites (ε units indicate the mass-independent isotope variations per 10,000 relative to terrestrial samples). This is because these mass-independent isotope variations are not affected by parent body processes. Hence, measuring the isotopic compositions of ungrouped chondrites is important for understanding their potential relationships with the established chondrite groups and expanding the number of likely chondrite parent bodies that are sampled by our collections (Clayton and Mayeda, 1984; Schiller et al., 2018; Trinquier et al., 2007; Zhang et al., 2012; Zhu et al., 2021b).

As firstly noted by Trinquier et al. (2007), Trinquier et al. (2009) and Warren (2011), all the carbonaceous (CC) chondrites and related achondrites (Göpel et al., 2015; Sanborn et al., 2019), have ε^{54}Cr, ε^{50}Ti and ε^{48}Ca values that are higher than those of the Earth-Moon system, while the non-carbonaceous (NC) meteorites: enstatite (ECs), ordinary (OCs), and Rumuruti (RCs) chondrites and the NC achondrites (e.g., aubrites, Martian meteorites, angrites and howardite-eucrite-diogenite clan) have terrestrial-like or negative ε^{54}Cr, ε^{50}Ti and ε^{48}Ca values (Dauphas et al., 2014; Göpel et al., 2015; Schiller et al., 2018; Shuai et al., 2022; Trinquier et al., 2007; Trinquier et al., 2009; Zhang et al., 2012; Zhu et al., 2021a; Zhu et al., 2021b). Currently, a number of models have been proposed for the isotopic differences between the CCs and NCs, including snow line migration (Lichtenberg et al., 2021), a ringed structure create by pressure maximum in the disk near Jupiter's location (Brasser and Mojzsis, 2020), or Jupiter formation (Kruijer et al., 2017).

A generally similar dichotomy for chondrites is seen in bulk O isotope anomalies, with the CCs having Δ^{17}O values below and the NCs similar to or above those of the Earth-Moon system (Javoy, 1995). Unlike chondrites, this dichotomy is less clear with some achondrites. The ureilites are C-rich achondrites with CC-like O isotope compositions (Goodrich, 1992). Hence, the ureilites were thought previously to derive from a CC-like parent body (Clayton and Mayeda, 1988). However, the nucleosynthetic isotopic anomalies in Cr (Qin et al., 2010b; Yamakawa et al., 2010; Zhu et al., 2020b), Ti (Trinquier et al., 2009), Ca (Chen et al., 2011; Schiller et al., 2018), Ni (Quitté et al., 2010) and Mo (Budde et al., 2019), all suggest that the ureilites belong to the NCs. At present, it is not clear whether the ureilite parent body accreted in the inner Solar System (Schiller et al., 2018; Schiller et al., 2020; Yamakawa et al., 2010) or the outer Solar System (Goodrich et al., 2015). By contrast, Northwest Africa [NWA] 011 is a C-free achondrite with a petrology that is similar to the eucrites (Yamaguchi et al., 2002), but its positive ε^{54}Cr signature (1.37 ± 0.04; 2SD, N = 2) (Warren, 2011) precludes a NC origin, at least as currently defined. Chondrites are thought to reflect the compositions of primitive building blocks of terrestrial planets and achondrite parent bodies (Allègre et al., 1995; Krot et al., 2014; McDonough and Sun, 1995), but ureilites, eucrites and diogenites possess more negative ε^{54}Cr, ε^{50}Ti and ε^{48}Ca values than any known chondrites (Chen et al., 2011; Schiller et al., 2018; Trinquier et al., 2007; Trinquier et al., 2009; Van Kooten et al., 2017; Yamakawa et al., 2010; Zhu et al., 2020b), suggesting that there should exist some unsampled chondrite reservoirs. Analyzing ungrouped chondrites and achondrites may expand the range of nucleosynthetic and O isotope anomalies, thereby testing the apparent existence of interelement correlations within and between the NC and CC families and, indeed, the CC-NC dichotomy itself.

Calcium is a major (with content of >1 wt%) refractory lithophile element in meteorites and most planetary igneous rocks, so it can be used for determining kinships (Dauphas et al., 2014; Schiller et al., 2018). The ε^{48}Ca literature values for the ECs (from −0.58 ± 0.40 to −0.22 ± 0.35, 2SE) overlap with those of the Earth, Moon, ordinary chondrites (OCs), angrites and eucrites (Dauphas et al., 2014), and the precision of the measurements is a factor of 6 – 10 times lower than more recent work based on improved techniques using plasma-based mass spectrometer (Lewis et al., 2022; Schiller et al., 2018). The isotopic similarities between the ECs and the Earth-Moon system, in particular, have been used to argue for EC-like material dominating the Earth's building blocks (e.g., Javoy et al., 2010; Mougel et al., 2018; Zhu et al., 2020a). Some new enstatite-rich meteorites/clasts have been recently reported, such as samples from the Almahata Sitta strewn field that are believed to come from a ~500 km asteroid, (Harries and Bischoff, 2020), EH7-anomalous Itqiy and NWA 2526 (Keil and Bischoff, 2008; Moynier et al., 2020; Patzer et al., 2001). Their relationships, if any, to the ECs and the Earth-Moon system are poorly understood. Investigating their ε^{48}Ca compositions by Multicollector Inductively Coupled Plasma Mass Spectrometry (MC-ICP-MS) can potentially provide information on their relationships to known meteorite groups and better test the Earth-EC connection. Additionally, the KC grouplet (Davis et al., 1977; Weisberg et al., 1996) lacks any nucleosynthetic isotope data.

Investigating the radiogenic Mg isotope compositions (reported as μ^{26}Mg*, the parts per million deviation of the normalized ^{26}Mg/^{24}Mg isotope ratios relative to a terrestrial standard) of bulk chondrites can shed light on the thermal histories of early Solar System planetesimals (Larsen et al., 2016a; Larsen et al., 2011; Luu et al., 2019). There is a positive correlation between μ^{26}Mg and ε^{54}Cr values for the solar system material, which is interpreted as reflecting progressive thermal processing of infalling ^{26}Al-rich molecular cloud material in the inner Solar System (Larsen et al., 2011; Van Kooten et al., 2016). However, this correlation is mostly controlled by the CAI-AOA components, and individual CCs do not fall on this correlation line (Luu et al., 2019). Hence, more combined μ^{26}Mg* and ε^{54}Cr data of chondrites are needed to further test this correlation and its significance.

Here, we report the bulk elemental ratios and high-precision mass-independent Cr, Ca and Mg isotope data for four enstatite meteorites, one KC, 17 ungrouped chondrites (three that have been classified as NCs and 14 as CCs) and two terrestrial samples. We also report the bulk ε^{48}Ca data for three enstatite-rich achondrite samples (Harries and Bischoff, 2020; Zhu et al., 2021c). We will discuss the significant implications of our results for the diversity of isotope reservoirs in the solar system, the NC-CC dichotomy, the classification for ungrouped chondrites, and for the early solar system chronology defined by chondrites.

2. Samples and analytical methods

2.1. Samples and digestion

This main focus of this study is to report Cr, Ca and Mg isotopic anomalies in ungrouped chondrites. Since the KC grouplet only

contains four members, as of 2021 (Gattacceca et al., 2021), and lack any published measurements of their mass-independent isotope compositions, we also selected one of them for analysis. Additionally, Itqiy (EH7) and some enstatite-rich clasts show similar ε^{54}Cr values, and possibly originate from a common parent body (Zhu et al., 2021c). We also determined their Ca and Mg isotope compositions to test this hypothesis. The sample suite analyzed in this study includes: 1) one EC, Sahara [SAH] 97096 (paired with SAH 97072 and many others); 2); one KC, Lewis Cliff [LEW] 87232; 3) three ungrouped NCs, Miller Range [MIL] 15362, Grosvenor Mountains [GRO] 95551, and NWA 5717; 4) 15 ungrouped CCs: Miller Range [MIL] 090292 (C1), MacAlpine Hills [MAC] 87300 (C2), Queen Alexandra Range (QUE) 99038 (C2), Bells (C2), MAC 87301 (C3), MAC 88107 (C3), Dar al Gani [DaG] 430 (C3), DaG 429 (C3), NWA 1152 (C3), NWA 12416 (C3), DaG 978 (C3), Buckley Island [BUC] 10933 (CR2), MIL 07513 (CR2), MIL 090001 (CR2), and Ningqiang (C3); and 5) Itqiy (Patzer et al., 2001), and two enstatite-rich stones (MS-MU-019 and MS-MU-036) (Bischoff et al., 2022; Harries and Bischoff, 2020) from the Almahata Sitta strewn field (Harries and Bischoff, 2020; Horstmann and Bischoff, 2014). Note that BUC 10933, MIL 07513 and MIL 090001 are currently classified as CR2 chondrites in the Meteoritical Bulletin, but their classifications are still under debate (Alexander et al., 2013). We also measured two terrestrial peridotites for data quality control. These two peridotites experienced carbonatite metasomatism (Hauri et al., 1993), and because of their resulting high Sr contents they are not suitable for standards of Ca isotope data determination using our Ca isolation protocols. All the sample information can be found in Table 1.

For each chondrite, 0.2–1 g chips were ground to powders, from which 30–100 mg aliquots were weighed for digestion. The samples were dissolved following the protocol described in Inglis et al. (2018) using Teflon bombs and an Analab EvapoClean that has been successfully used in previous studies (Zhu et al., 2019b; Zhu et al., 2021b; Zhu et al., 2021c; Zhu et al., 2020b). The procedure involved heating the samples in concentrated HF and HNO_3 (2:1) at 140 ℃ for two days, drying down the samples and subsequent dissolution of the solid residues in 6 M HCl (also at 140 ℃) for another two days to ensure complete digestion of fluorides, and refractory phases such as chromite and spinel. No visible particles could be seen in the solutions, except the C phases on the beaker walls. After digestion, all the samples were dissolved in 1 mL of 6 M HCl. Ten percent (100 µl) of each solution was preserved for measurements of elemental concentrations. Roughly 5 mg of each solution was taken for mass-independent Cr isotope analysis, using the method described in Zhu et al. (2021b). A separate 10–20 mg of each solution was taken for mass-independent Ca and Mg isotope analysis, followed the methods described in Schiller et al. (2015b) and Bizzarro et al. (2011) respectively.

2.2. $^{27}Al/^{24}Mg$ and $^{55}Mn/^{52}Cr$ ratio measurements

The element concentrations in the solutions were determined with an Agilent 7900 quadrupole inductively coupled plasma mass spectrometer (ICP-MS) housed at the Institut de Physique du Globe de Paris (IPGP). Elements with masses between that of Na (23) and As (75), as well as Ag (107), Cd (111) and Gd (157), were measured using a collision-reaction cell with helium gas (5 mL/min) to remove polyatomic interferences. All other elements were measured without collision gas. Sc, In and Rh internal-standards were injected after inline mixing with the samples to correct for signal drift and matrix effects. Two sets of multi-element calibration standards (one for major and one for trace elements) were analyzed to confirm and model (through simple linear regression) the linear relationship between signal and concentration. The model was then used to convert measured sample counts to concentrations. Reported uncertainties were calculated using error propagation equations and considering the combination of standard deviations on replicated consecutive signal acquisitions (n = 3), internal-standard ratio and blank subtraction. The non-linear term (internal-standard ratio) was linearized using a first-order Taylor series expansion to simplify error propagation. $^{27}Al/^{24}Mg$ ratios were directly calculated from the Al and Mg concentrations. The upper limit of two standard deviation uncertainties (2SD) precision for the $^{27}Al/^{24}Mg$ ratios were estimated to be 5 % based on multiple measurements of BE-N (0.764 ± 0.021; 2SD, N = 3), BHVO-2 (1.866 ± 0.005; 2SD, N = 3) and BCR-2 (3.761 ± 0.024; 2SD, N = 4).

We employed a Neptune Plus MC-CP-MS to measure the $^{55}Mn/^{52}Cr$ ratios. The detailed method was described in Zhu et al. (2021b). The 2σ uncertainties in the $^{55}Mn/^{52}Cr$ ratios were estimated to be 2 %, based on multiple measurements of DTS-1 (0.228 ± 0.002), PCC-1 (0.353 ± 0.002, N = 7) and BHVO-2 (5.173, N = 1) and comparison with literature data (Qin et al., 2010a; Trinquier et al., 2008b).

2.3. Cr isotope measurements

To chemically purify Cr, we used a four-step column chemistry described in Zhu et al. (2021b). We first used an anion chromatographic purification scheme to efficiently remove Fe from the remaining sample in 6 M HCl, followed by elution of Cr on a 1 mL cation exchange column in 20 mL of 0.5 M HNO_3 to remove the major elements including Mg, Ca, Al, Ni (Bizzarro et al., 2011) and collect all the Cr species (major Cr^0 and minor Cr^{2+} and Cr^{3+}) to reach an ~100 % recovery. Prior to sample loading on the cation column, we used a Cr pre-treatment procedure involving dissolution in 10 M HCl at > 120 °C to efficiently promote the formation of Cr(III)-Cl species, which have a low affinity for the cation exchanger and thus elutes early (Larsen et al., 2016b; Trinquier et al., 2008a). The third clean-up column involved Cr purification from Al, Fe, V, and Ti (and other high-field-strength elements) and Mn, Na, and K on a small (0.33 mL) cation exchange column using 0.5 M HNO_3, 1 M HF and 6 M HCl (Larsen et al., 2018). Prior to sample loading onto this last column, we used a Cr pre-treatment procedure involving exposure to 0.5 M HNO_3 + 0.6 % H_2O_2 at room temperature for > 1 day to promote the formation of Cr^{3+} (Larsen et al., 2016). However, it is difficult to transform all the Cr to Cr^{3+}, so we collect the Cr^0, Cr^+, and Cr^{2+} in 0.5 mL solution of sample loading and 0.5 mL 0.5 M HNO_3 elution to increase the recovery to > 95 % in this column. Finally, in the fourth column, 0.7 mL of TODGA resin was used in 8 M HCl to remove the residual Fe, V, and Ti, which are isobars for ^{54}Cr (^{54}Fe) and ^{50}Cr (^{50}V and ^{50}Ti) (Pedersen et al., 2019). The four columns can reach a total yield between 95 % and 99 %, and effectively remove Fe, V, and Ti, which benefits the isotope analysis by MC-ICP-MS. The total blank of <5 ng is negligible compared to the 15–20 µg of Cr processed through the columns. The final Cr solutions were redissolved in 100 µl of concentrated HNO_3 and then dried again 2–3 times to transform the acid media and to minimize residual organics (i.e., from the cation exchange resin).

The Cr isotopic compositions were determined using a Neptune Plus MC-ICP-MS located at the Centre for Star and Planet Formation, Globe Institute, University of Copenhagen. Detailed analytical and data reduction method are described in (Zhu et al., 2021b). Sample solutions with concentrations of 0.5–1 ppm were introduced via an ESI APEX desolvating nebulizer and analyzed at a ^{52}Cr signal of 30–40 V, and the signals of samples always match those of NIST 979 standard within 5 % uncertainty. Each sample was measured five times by sample-standard bracketing relative to the NIST SRM 979 Cr standard. The $^{53}Cr/^{52}Cr$ and $^{54}Cr/^{52}Cr$ ratios were normalized to a constant $^{50}Cr/^{52}Cr$ ratio of 0.051859 using an

Table 1
Cr and Ca isotope data for enstatite, Kakangari and ungrouped chondrites.

Samples NameNa	Type	Total Mass (g)	$^{55}Mn/^{52}Cr$	error	**$\varepsilon^{53}Cr$**	2se	**$\varepsilon^{54}Cr$**	2se	N	**$\varepsilon^{43}Ca$**	**2SE**	**$\varepsilon^{48}Ca$**	2SE	N	**$\Delta^{17}O$#**	Error	**$\varepsilon^{50}Ti$#**	2se
SAH 97096	EH3	0.0332	0.650	0.013	**0.25#**	0.03	**0.17#**	0.08	5	0.02	0.07	**−0.19**	0.22	5				
LEW 87232	K	0.0457	1.322	0.026	**0.50**	0.02	**−0.44**	0.04	5	−0.03	0.05	**−1.30**	0.25	4	**−1.22**	0.08		
MIL 15362	Ungrouped/H4-an	0.0487	0.593	0.012	**0.18**	0.02	**−0.37**	0.05	5	0.01	0.10	**−0.83**	0.17	5				
GRO 95551	Ungrouped	0.0724	0.397	0.008	**0.01**	0.03	**−0.07**	0.08	5	0.00	0.06	**−0.40**	0.03	5	**0.49**	0.08		
NWA 5717	Ungrouped 3.05	0.0454	0.705	0.014	**0.22**	0.02	**−0.34**	0.10	5						**0.57**	0.08	**−0.61**	0.07
MIL 090292	Ungrouped C1/CR1				**0.14**	0.02	**1.26**	0.04	5						**−2.21**	0.77		
MAC 87300	Ungrouped C2	0.1075	0.491	0.010	**0.09**	0.02	**0.74**	0.05	5	0.12	0.03	**3.16**	0.12	5	**−4.93**	0.05	**4.67**	0.15
MAC 87301	Ungrouped C3	0.0577	0.475	0.010	**0.10**	0.03	**0.81**	0.05	5	0.14	0.02	**3.17**	0.11	5	**−4.79**	0.06	**4.12**	0.15
MAC 88107	Ungrouped C3	0.0500	0.470	0.009	**0.11**	0.03	**0.68**	0.04	5						**−4.63**	0.03	**3.13**	0.15
QUE 99038	Ungrouped C2/CM2/CV3	0.0371	0.401	0.008	**0.06**	0.01	**0.92**	0.01	5	0.13	0.03	**2.83**	0.21	5				
Tagish Lake	Ungrouped C2		1.690	0.020	**0.53#**	0.05	**1.19#**	0.10				**2.91#**	0.05		**−0.87**	0.54	**2.76**	0.26
Bells	Ungrouped C2	0.0358	0.556#	0.011	**0.15**	0.01	**1.23**	0.07	5	0.11	0.03	**1.94**	0.13	5	**−1.90**	0.08		
DaG 430	Ungrouped C3	0.0342	0.424	0.008	**0.04**	0.02	**0.75**	0.04	5	0.09	0.05	**2.31**	0.17	5	**−4.52**	0.08		
DaG 429	Ungrouped C3	0.0446	0.389	0.008	**0.02**	0.04	**0.69**	0.03	5	0.07	0.06	**2.28**	0.17	5				
DaG 978	Ungrouped C3	0.0388	0.385	0.008	**0.09**	0.03	**0.86**	0.08	5	0.13	0.05	**2.47**	0.20	5				
NWA 1152	Ungrouped C3	0.0426	0.424	0.008	**0.10**	0.02	**0.72**	0.04	5	0.11	0.08	**2.03**	0.20	5	**−3.77**	0.03		
NWA 12416	Ungrouped C3	0.0500	0.580	0.012	**0.17**	0.03	**1.40**	0.05	5	0.11	0.05	**0.28**	0.29	5	**−5.93**	2.66		
BUC 10933	Ungrouped C2/CR2	0.0332	0.396	0.008	**0.07**	0.04	**0.86**	0.05	5	0.12	0.03	**3.07**	0.10	5				
MIL 07513	Ungrouped C2/CR2	0.0334	0.422	0.008	**0.11**	0.03	**0.93**	0.07	5	0.25	0.03	**3.91**	0.07	5				
MIL 090001	Ungrouped C2/CR2	0.0370	0.529	0.010						0.12	0.11	**2.46**	0.11	5				
Ningqiang	Ungrouped C3	0.0569			**0.11**	0.03	**0.75**	0.08	10*						**−4.55**	0.08		
Flensburg	Ungrouped C1				**0.20#**	0.04	**0.95#**	0.05	17								**3.31**	0.08
Itqiy	EH7-an (Bulk)									−0.01	0.02	**−0.40**	0.13	5				
Itqiy	EH7-an				**0.52#**	0.04	**−0.27#**	0.10	13*	−0.02	0.03	**−0.29**	0.13	5				
MS-MU-019	Enstatite achondrite clast				**1.76#**	0.04	**−0.25#**	0.08	11*	−0.01	0.03	**−0.32**	0.07	5				
MS-MU-036	Enstatite achondrite clast									0.03	0.07	**−0.38**	0.17	5				
SAV 1-1	Terrestrial peridotite	0.0297			**0.02**	0.02	**0.06**	0.07	5									
TBA 1-9	Terrestrial peridotite	0.0374			**0.02**	0.02	**0.02**	0.07	5									

Note: # indicates literature data, and these include all the $\Delta^{17}O$ and $\varepsilon^{50}Ti$ data, and some of the Cr data. $\Delta^{17}O$ data sources: (Clayton and Mayeda, 1999; Greenwood et al., 2020; Schrader et al., 2014; Torrano et al., 2021) and Meteoritical Bulletin; $\varepsilon^{50}Ti$ data source: (Bischoff et al., 2021; Torrano et al., 2021); $\varepsilon^{54}Cr$ data source: (Bischoff et al., 2021; Petitat et al., 2011; Zhu et al., 2021b; Zhu et al., 2021c). The Cr isotope data marked with * were measured by total evaporation method on TIMS, and the method is described in Zhu et al. (2021c). We also report the $\varepsilon^{46}Ca$ data (with large uncertainty) in supplementary material (Table S1).

exponential law (Lugmair and Shukolyukov, 1998) and are expressed in the epsilon notation:

$$\varepsilon^{x}Cr = \left(\frac{(^{x}Cr/^{52}Cr)_{sample}}{(^{x}Cr/^{52}Cr)_{NIST\ SRM\ 979}} - 1\right) \times 10,000, \quad (1)$$

with x = 53 or 54.

2.4. Ca isotope measurements

Calcium was separated from the sample aliquots by ion-exchange chromatography in a four-step procedure following the protocol described in (Schiller et al., 2018; Schiller et al., 2015a). Individual chromatography separation steps were repeated when the presence of contaminants could affect the analysis (for example, when the Sr/Ca ratio was higher than 1×10^{-6}). The Ca isotopic compositions for which sufficient Ca was available were measured with a Neptune Plus MC-ICP-MS at the Centre for Star and Planet Formation, Globe Institute, University of Copenhagen relative to the NIST SRM 915b Ca standard. Data were acquired in the static mode using six Faraday collectors, one for each of the isotopes ^{48}Ca, ^{47}Ti, ^{46}Ca, ^{42}Ca, ^{43}Ca and ^{44}Ca. The Faraday cup used for ^{47}Ti was connected to an amplifier with a 10^{12} Ω feedback resistor, whereas the other collectors were connected to amplifiers with 10^{11}-Ω feedback resistors. Samples were aspirated into the plasma source by means of an Apex sample introduction system with an uptake rate of 20 µl min^{-1}, and the Ca isotopes were measured at medium resolution, with a mass resolving power ($M/\Delta M$, as defined by the peak edge width from 5 % to 95 % at full peak height) that was always >5,000. Calcium concentrations with 5–8 ppm under these analytical conditions (i.e., uptake rate, resolution, etc.) gave total Ca signals of 750–1250 V. An individual measurement was comprised of 100 cycles with integration times of 8.4 s, followed by 340 s of baseline measurements. Each sample measurement was bracketed by measurements of SRM 915b. All sample measurements were repeated five times. The ^{48}Ca/^{44}Ca ratio was normalized to a constant ^{42}Ca/^{44}Ca ratio of 0.31221, using an exponential law and is expressed in the epsilon notation:

$$\varepsilon^{48}Ca = \left(\frac{(^{48}Ca/^{44}Ca)_{sample}}{(^{48}Ca/^{44}Ca)_{NIST\ SRM\ 915b}} - 1\right) \times 10,000. \quad (2)$$

The data reduction was conducted off-line using Iolite 4 and changes in mass bias with time were interpolated using a smoothed cubic spline. For each analysis, the mean and standard error of the measured ratios were calculated using a two-standard-deviation threshold to reject outliers. The final uncertainties reported here are twice the standard error of the mean of the repeat analyses.

2.5. Mg isotope measurements

The purification of Mg followed an established column chromatography protocol as described in Bizzarro et al. (2011). Purified Mg samples were typically analysed with a signal intensity of 20–45 V on mass ^{24}Mg and each sample was systematically analysed 10 times. Mass-dependent Mg isotope data are reported in the δ-notation as deviations from the DSM3 using DTS-2b standard ($\delta^{25}Mg_{DSM3}$ = -0.122 ± 0.017 ‰ (2SD, Bizzarro et al., 2011) according to the following formula:

$$^{x}Mg = \left(\frac{(^{x}Mg/^{24}Mg)_{sample}}{(^{x}Mg/^{24}Mg)_{DTS-2b}} - 1\right) \times 1000, \quad (3)$$

where x = 25 or 26.

The mass-independent component of ^{26}Mg (µ ^{26}Mg*) is reported in the same fashion, but represents parts per million (ppm) deviations from the internally normalized ^{26}Mg/^{24}Mg of the sample from the reference standard, normalized to ^{25}Mg/^{24}Mg = 0.126896, using the exponential mass fractionation law (Bizzarro et al., 2011). All Mg data reduction was conducted off-line using the Iolite 4. Within this software, changes in mass bias with time were interpolated using a smoothed cubic spline. For each analysis, the mean and standard error of the measured ratios were calculated using a two-standard-deviation threshold to reject outliers. Individual analyses of a sample were combined to produce an average weighted by the propagated uncertainties of individual analyses and reported final uncertainties are the 2SE of the mean. The external reproducibility of our measurements using this method is 20 and 2.5 ppm for the δ ^{25}Mg and µ ^{26}Mg*, respectively Bizzarro et al. (2011).

3. Results

The detailed Cr and Ca isotope data are reported in Table 1, while the Mg isotope data are reported in Table 2. The measurements of the two terrestrial peridotite xenoliths produced isotopic compositions that are consistent with previous measurements of terrestrial ε^{53}Cr, ε^{54}Cr (Mougel et al., 2018; Qin et al., 2010a; Trinquier et al., 2007; Trinquier et al., 2008b; Yamakawa et al., 2009; Zhu et al., 2021b) and μ^{26}Mg* values (Larsen et al., 2011; Luu et al., 2019; Van Kooten et al., 2016), confirming the accuracy of the Cr and Mg isotope data in this study. However, the two samples contain carbonates that are rich in Sr, which created isobaric interferences on the Ca mass array. The column chemistry we used cannot totally remove the Sr, so we do not report their ε^{48}Ca data. The ε^{54}Cr data for MAC 87300, MAC 87301, and MAC 88107 are also consistent with literature data (Torrano et al., 2021), albeit with a higher precision (∼0.06 vs ∼0.14; 2SE).

The ε^{54}Cr and ε^{48}Ca values for the ungrouped chondrites and KC (LEW 87232) vary from −0.44 ± 0.04 to 1.40 ± 0.05, and −1.30 ± 0.25 to 3.91 ± 0.07, respectively (Fig. 1). All the ungrouped CCs show positive ε^{54}Cr (>0.68) and ε^{48}Ca (>0.28) values, while the ungrouped NCs and the KC show negative or close-to-zero ε^{54}Cr and ε^{48}Ca values. SAH 97096 (EH3) possesses an ε^{48}Ca value of −0.19 ± 0.22, and LEW 87232 (K) has ε^{54}Cr and ε^{48}Ca values of −0.44 ± 0.04 and −1.30 ± 0.25, respectively. Itqiy (EH7) and the two enstatite-rich samples, MS-MU-019 and MS-MU-036, show homogenous ε^{48}Ca values, averaging at −0.35 ± 0.10 (2SD, N = 4). The relationships between ε^{54}Cr, ε^{48}Ca, ε^{50}Ti and Δ^{17}O values are shown in Fig. 2. The correlation between ε^{54}Cr and ε^{48}Ca is similar to that between ε^{54}Cr and ε^{50}Ti (Fig. 2).

LEW 87232 has a solar-like ^{27}Al/^{24}Mg ratio of 0.104 and a μ^{26}Mg* of −4.0 ± 1.8, while MIL 07513 (Ungrouped C2/CR2) has an anomalously high ^{27}Al/^{24}Mg ratio, corresponding to a high μ^{26}Mg* value of 39.0 ± 2.6. Some chondrites, e.g., MIL 15362 (ungrouped), GRO 95551 (ungrouped), MAC 87301 (C3) and MAC 88107 (C3), with similar ^{27}Al/^{24}Mg ratios of ∼0.19 have different μ^{26}Mg* values ranging from −0.3 ± 2.5 to 19.0 ± 2.3. There is no significant linear correlation of ^{27}Al/^{24}Mg – μ^{26}Mg* for the chondrites, when combined with literature data (Larsen et al., 2011; Luu et al., 2019; van Kooten et al., 2020) (2SE, MSWD = 21, N = 50; Fig. 3), but there is a positive trend. If regressing them as a linear correlation with slope of 162.8 ± 49.2 and a y-axis intercept of −16.0 ± 5.5 when using a model 3 (due to MSWD ≫ 1) fit with IsoplotR (Vermeesch, 2018).

Most of the chondrites have ^{55}Mn/^{52}Cr ratios in the range 0.4 – 0.8, while LEW 87232 (KC), possesses a high ^{55}Mn/^{52}Cr ratio of 1.32 and a correspondingly high ε^{53}Cr value of 0.50 ± 0.02. All the ungrouped chondrites and the KC in this study fall on a ^{55}Mn/^{52}Cr – ε^{53}Cr correlation line (Fig. 4), with a slope of 0.484 ± 0.051 (2σ; MSWD = 4.2; N = 16) and intercept (y-axis) of −0.13 ± 0.03, also using a model 3 (due to MSWD ≫ 1) fit with IsoplotR (Vermeesch, 2018).

Table 2
^{26}Al-^{26}Mg and Mg isotope data for the chondrites.

Sample	Type	^{27}Al/^{24}Mg	Error (5 %)	**μ^{26}Mg***	2SE	δ^{25}Mg	**δ^{25}Mg$_{-DSM}$**	2SD	2SE	δ^{26}Mg	2SE	N
SAH 97096	EH3	0.085	0.004	**−1.4**	1.4	−0.03	**−0.15**	0.06	0.02	−0.05	0.04	10
LEW 87232	K	0.104	0.005	**−4.0**	1.8	0.00	**−0.12**	0.05	0.02	−0.01	0.03	10
MIL 15362	Ungrouped/H4-an	0.185	0.009	**−0.3**	2.5	−0.05	**−0.17**	0.06	0.02	−0.10	0.03	10
GRO 95551	Ungrouped	0.194	0.010	**0.6**	2.5	−0.09	**−0.21**	0.04	0.01	−0.17	0.02	10
NWA 5717	Ungrouped 3.05	0.091	0.005	**−1.3**	2.6	−0.06	**−0.19**	0.10	0.03	−0.13	0.06	10
MAC 87300	Ungrouped C2	0.118	0.006	**12.9**	2.1	−0.11	**−0.23**	0.09	0.03	−0.21	0.05	10
MAC 87301	Ungrouped C3	0.204	0.010	**9.8**	2.4	−0.05	**−0.17**	0.03	0.01	−0.08	0.02	10
MAC 88107	Ungrouped C3	0.192	0.010	**19.0**	2.3	−0.03	**−0.15**	0.04	0.01	−0.03	0.03	10
QUE 99038	Ungrouped C2/CM2/CV3	0.130	0.007	**8.2**	2.7	0.06	**−0.06**	0.03	0.01	0.13	0.02	10
Bells	Ungrouped C2	0.096	0.005	**−6.6**	1.8	0.00	**−0.12**	0.09	0.03	−0.01	0.06	10
DaG 430	Ungrouped C3	0.103	0.005	**4.6**	1.9	0.01	**−0.11**	0.12	0.04	0.03	0.07	10
DaG 429	Ungrouped C3	0.112	0.006	**2.5**	1.2	−0.02	**−0.15**	0.09	0.03	−0.04	0.06	10
DaG 978	Ungrouped C3	0.134	0.007	**7.3**	2.5	0.01	**−0.12**	0.06	0.02	0.02	0.04	10
NWA 1152	Ungrouped C3	0.113	0.006	**2.2**	2.0	−0.01	**−0.13**	0.03	0.01	−0.02	0.02	10
NWA 12416	Ungrouped C3	0.124	0.006	**7.0**	1.5	−0.05	**−0.18**	0.06	0.02	−0.10	0.04	10
BUC 10933	Ungrouped C2/CR2	0.146	0.007	**9.3**	2.0	−0.04	**−0.16**	0.05	0.02	−0.07	0.03	10
MIL 07513	Ungrouped C2/CR2	0.310	0.016	**39.0**	2.6	−0.02	**−0.14**	0.07	0.02	0.01	0.04	10
MIL 090001	Ungrouped C2/CR2	0.125	0.006	**−4.7**	1.4	0.01	**−0.12**	0.06	0.02	0.01	0.04	10
SAV-1–1	Terrestrial peridotite	0.04	0.00	**3.2**	2.7	−0.03	**−0.15**	0.06	0.02	−0.06	0.04	10
TBA 1–9	Terrestrial peridotite	0.10	0.01	**0.6**	1.8	0.00	**−0.12**	0.11	0.04	0.01	0.07	10

Note: μ^{26}Mg* represents parts per million (ppm) deviations from the internally normalized ^{26}Mg/^{24}Mg of the sample from the reference standard, normalized to ^{25}Mg/^{24}Mg = 0.126896, using the exponential mass fractionation law.

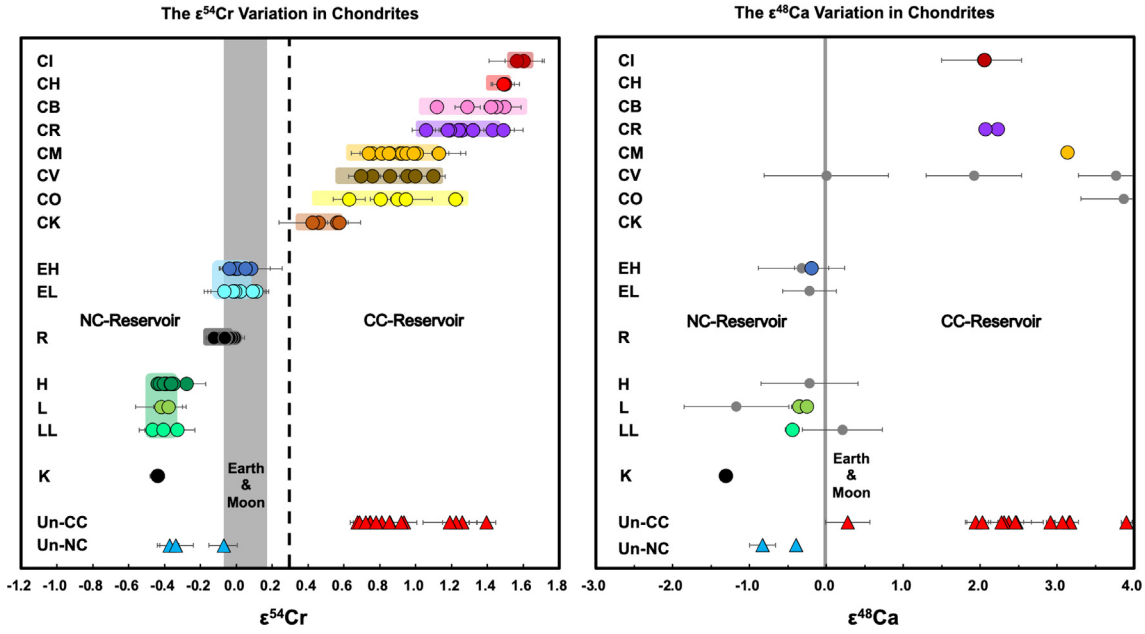

Fig. 1. The ε^{54}Cr and ε^{48}Ca compositions of ungrouped chondrites and other Solar System materials (literature ε^{48}Ca measured by TIMS were shown as small grey circles). Red triangles are ungrouped carbonaceous chondrites (Un-CCs), and the blue triangles are the ungrouped non-carbonaceous chondrites (Un-NCs). The grey bars represent the Earth and Moon values. It can be seen that all the Un-CCs and Un-NCCs have positive and negative ε^{54}Cr and ε^{48}Ca values, respectively. Literature data: ε^{54}Cr (Qin et al., 2010a; Schiller et al., 2018; Schiller et al., 2015b; Trinquier et al., 2007; Zhu et al., 2021a; Zhu et al., 2021b); ε^{48}Ca (Dauphas et al., 2014; Moynier et al., 2010; Schiller et al., 2018; Schiller et al., 2015b). Note: in Dauphas et al. (2014), some ε^{48}Ca data measured respectively in multidynamic and static modes are not consistent. Here, we cited the data from multidynamic measurements; we did not cite the ε^{48}Ca data with uncertainty > 1 in Moynier et al. (2010). (For interpretation of the references to colour in this figure legend, the reader is referred to the web version of this article.)

4. Discussion

4.1. Cr and Ca isotope compositions

Unlike some chondrite groups, e.g., CVs, COs and CMs (Fig. 1) that show large intra-group ε^{54}Cr and ε^{50}Ti heterogeneities (Trinquier et al., 2009; Zhang et al., 2012; Zhu et al., 2021b), the ECs have ε^{54}Cr and ε^{50}Ti values that fall in a restricted range (Zhang et al., 2012; Zhu et al., 2021b). Hence, the ε^{48}Ca values for bulk ECs could also be homogeneous, and one EC sample may well be representative of the ε^{48}Ca isotope compositions for all ECs. In this study, the ε^{48}Ca value for SAH 97096 (−0.19 ± 0.22, 2SE) is consistent with previous ε^{48}Ca data (Dauphas et al., 2014), albeit with better precision. SAH 97096 has the same ε^{48}Ca value, within error, as that of Earth (0.00 ± 0.11, 2SD) and the Moon (0.04 ± 0.04, 2SD) (Schiller et al., 2018; Schiller et al., 2015b). The ε^{48}Ca similarity between the ECs and the Earth-Moon system is consistent with their ε^{54}Cr and Δ^{17}O (per 1000 deviation from terrestrial samples for mass-independent O isotope fractionation) isotope systematics (Clayton et al., 1984; Mougel

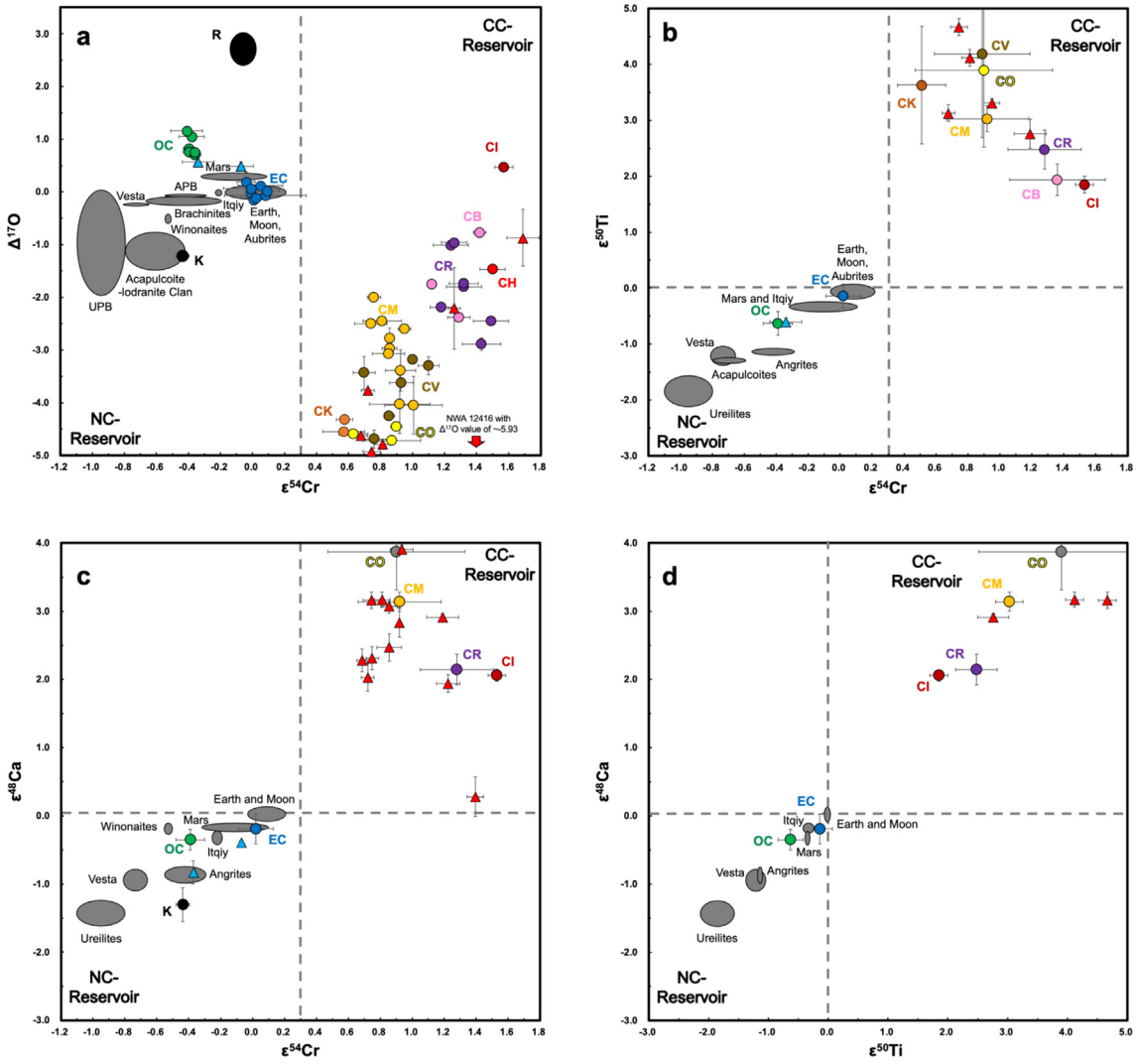

Fig. 2. The relationships between $\Delta^{17}O$, $\varepsilon^{54}Cr$, $\varepsilon^{50}Ti$ and $\varepsilon^{48}Ca$ for the Solar System materials. Colorful circles are chondrites, same as those in Fig. 1, while the grey areas represent the differentiated planetesimals and planets. The dashed lines are the boarders of CC and NC material. Literature data: $\Delta^{17}O$ (Greenwood et al., 2017; Torrano et al., 2021) and Meteoritical Bulletin, $\varepsilon^{54}Cr$ (Qin et al., 2010a; Trinquier et al., 2007; Zhu et al., 2019b; Zhu et al., 2021a; Zhu et al., 2021b; Zhu et al., 2021c; Zhu et al., 2020b; Zhu et al., 2022), $\varepsilon^{50}Ti$ (Torrano et al., 2021; Trinquier et al., 2009; Zhang et al., 2012) and $\varepsilon^{48}Ca$ (Dauphas et al., 2014; Schiller et al., 2018; Schiller et al., 2015b). Note: we use grey circles to represent the $\varepsilon^{48}Ca$ data of CO chondrites in Dauphas et al. (2014), due to the relatively large data uncertainty of the TIMS measurements. The $\varepsilon^{48}Ca$ data of CV chondrites are not consistent between Moynier et al. (2010) and Dauphas et al. (2014), ranging from ~0 to ~3.8 (also Fig. 1), so we did not show them in these figures.

et al., 2018; Qin et al., 2010a; Trinquier et al., 2007; Zhu et al., 2020a), supporting a similar isotopic composition between the ECs and Earth materials for these elements (Javoy et al., 2010; Moynier and Fegley Jr, 2015). The $\varepsilon^{48}Ca$ value for SAH 97096 also overlaps with those of the OCs (−0.35 ± 0.15, 2SD) (Dauphas et al., 2014; Schiller et al., 2018; Schiller et al., 2015b), which is not consistent with other isotope system, e.g., ^{50}Ti that was assumed to has same isotopic carrying phase as ^{48}Ca. Hence, more precise $\varepsilon^{48}Ca$ data for ECs are needed for possibly detecting a $\varepsilon^{48}Ca$ gap between ECs and OCs.

Itqiy (EH7) has a similar $\varepsilon^{48}Ca$ value to those of the two enstatite-rich stones from the Almahata Sitta strewn field, which is consistent with their similar $\varepsilon^{54}Cr$ values (Zhu et al., 2021c). The three samples, possibly representing the Itqiy parent body, give an average $\varepsilon^{48}Ca$ value of −0.35 ± 0.10 (2SD, N = 4). This value is clearly lower than that of the Earth-Moon system and similar to that of the EH3 chondrite ($\varepsilon^{48}Ca$ = -0.19 ± 0.22). This combined with their $\varepsilon^{54}Cr$ (−0.26 ± 0.03, 2SD, N = 2) and $\varepsilon^{50}Ti$ data (−0.34 ± 0.03, 2SD; two replicate measurements for Itqiy) (Trinquier et al., 2009; Zhu et al., 2021c) suggests that Itqiy is not an EH, but came from a distinct EC-like parent body. Although the $\varepsilon^{48}Ca$ values for the Itqiy parent body is consistent with that of the OCs (−0.35 ± 0.15), any genetic relationship can be excluded due to their distinct $\varepsilon^{54}Cr$, $\varepsilon^{50}Ti$ and $\Delta^{17}O$ compositions (Patzer et al., 2001; Trinquier et al., 2009; Zhu et al., 2021c).

The KCs are a rare grouplet (Davis et al., 1977; Weisberg et al., 1996). LEW 87232 has $\varepsilon^{54}Cr$ value of −0.44 ± 0.04 that is the same within uncertainty as that of the OCs with $\varepsilon^{54}Cr$ −0.39 ± 0.10 (2SD) (Pedersen et al., 2019; Qin et al., 2010a; Trinquier et al., 2007), but they do not share common $\Delta^{17}O$ and $\varepsilon^{48}Ca$ compositions (Fig. 2), with ~-1.2 ‰ and −1.30 ± 0.25 for LEW 87232 (Weisberg et al., 1996) and 0.7 – 1.2 ‰ and −0.35 ± 0.15 for OCs, respectively (Clayton et al., 1991). Therefore, a direct genetic relationship between the KC and the OCs is unlikely.

Based on our data (Fig. 1), all the ungrouped CCs have $\varepsilon^{54}Cr$ values > 0.3, while the three ungrouped NCs and the one KC (belongs to NC) possess $\varepsilon^{54}Cr$ values that are lower than 0.3. Note that, the $\varepsilon^{54}Cr$ = 0.3 is usually set as the boundary of between the CCs and NCs (Zhu et al., 2021a; Zhu et al., 2021b), because some terrestrial samples have reported $\varepsilon^{54}Cr$ values of up to 0.2

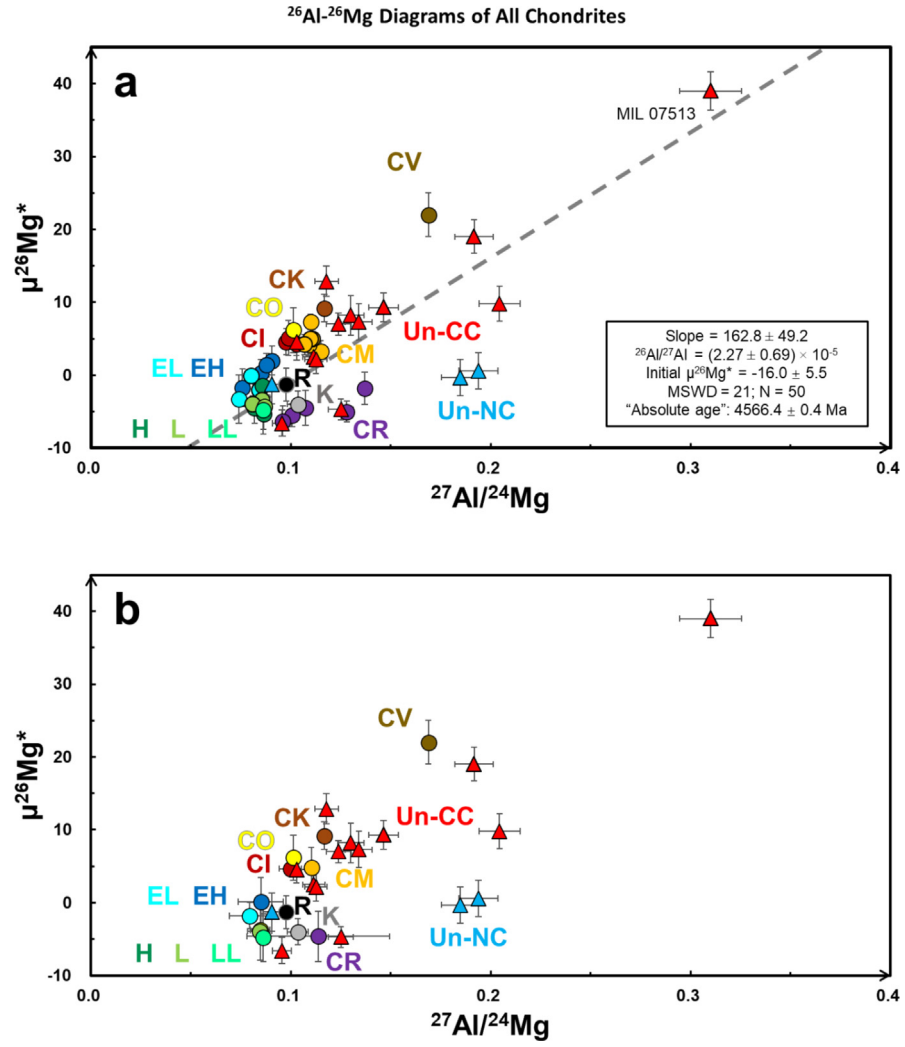

Fig. 3. ^{26}Al-^{26}Mg plots for chondrites. (a) and (b) are for individual chondrites and chondrite group average, respectively. The graphic symbols are the same as previous figures. These is no correlation between Al/Mg ratios and μ^{26}Mg* data. Literature data: (Larsen et al., 2011; Luu et al., 2019; van Kooten et al., 2020; Van Kooten et al., 2016).

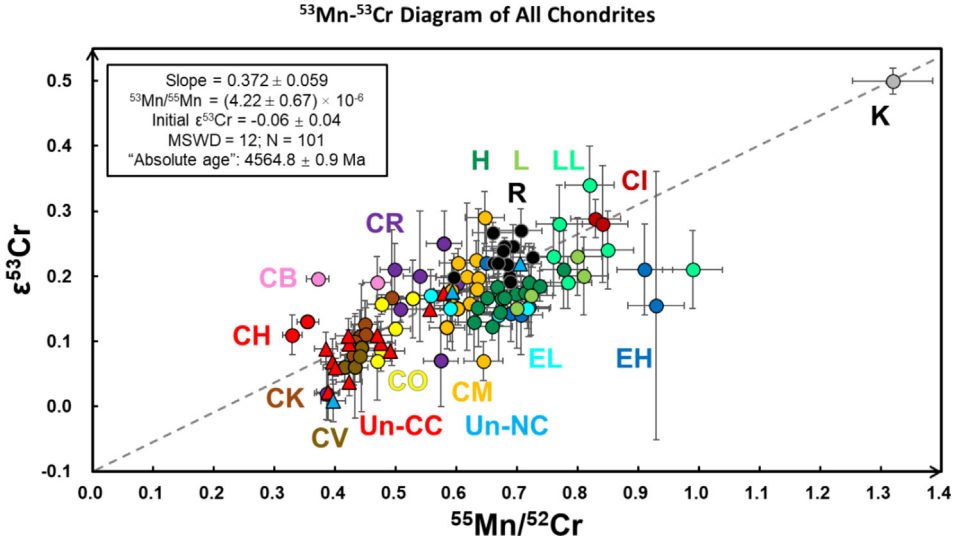

Fig. 4. ^{53}Mn-^{53}Cr plots for chondrites. The large MSWD (12) indicates that there is no well-defined Mn-Cr correlation line for all the chondrites if ε^{53}Cr anomalies were solely due to the decay of short-lived ^{53}Mn. The positive trend should only reflect mixing of several high and low Mn/Cr reservoirs (e.g., chondrules, matrix, CAIs, AOAs and metals). More detailed discussion can be found in Zhu et al. (2021b) and Zhu et al. (2021a), with literature data sources (Göpel et al., 2015; Qin et al., 2010a; Trinquier et al., 2008b; Zhu et al., 2021a; Zhu et al., 2021b).

(Mougel et al., 2018), and there is no ε^{54}Cr value for CCs lower than 0.4 (Zhu et al., 2021b). All the three ungrouped NCs and the one KC possess negative ε^{48}Ca values (at most −0.4), while all the ungrouped CCs have positive ε^{48}Ca values (>0.28). Note that NWA 12416 has the lowest ε^{48}Ca (0.28 ± 0.29) and Δ^{17}O (−5.93 ± 2.66; 2SD) values among chondrites, so it may need more petrological studies to figure out the origin for its extreme isotope compositions. Both the ε^{54}Cr and ε^{48}Ca systematics of the ungrouped chondrites are consistent with the CC-NC isotopic dichotomy.

The anomalous ε^{54}Cr, also ε^{48}Ca and ε^{50}Ti, compositions for ureilites (Chen et al., 2011; Qin et al., 2010b; Schiller et al., 2015b; Trinquier et al., 2009; Yamakawa et al., 2010; Zhu et al., 2020b) and NWA 011 (Warren, 2011) suggest the CC-NC dichotomy is more related to the petrology (mainly for chondrites) and isotope compositions (Kleine et al., 2020) rather than to the carbon contents (Mason, 1963) for chondrites. In detail, although most of CCs have higher carbon contents than OCs and ECs with petrological types of 3, some CCs, with petrologic types ≥ 3, possess similar carbon contents as ECs and OCs (Mostefaoui et al., 2000; Otting and Zähringer, 1967), which suggests thermal metamorphism had depleted the carbon contents in the meteorites. Also it should be noted that ureilites, with carbon contents ranging from 3 wt% to 7 wt% (Goodrich et al., 2015), experienced partial differentiation (Cohen et al., 2004). Since magmatic differentiation processes decrease the carbon content, the ureilite precursor was likely more carbon-rich than most CCs (e.g., CI chondrites have a carbon content of ~3.19 %) (Otting and Zähringer, 1967).

4.2. Suggestions of potential associations of the ungrouped chondrites

Combining Δ^{17}O, ε^{54}Cr, ε^{50}Ti and ε^{48}Ca values is a robust method for classifying chondrites. For example, MIL 15362 and NWA 5717 have OC-like ε^{54}Cr values (Zhu et al., 2021b), but their Δ^{17}O, ε^{50}Ti and ε^{48}Ca values (they do not share common isotope compositions) do not overlap with those of the OCs. Hence, they must originate from parent bodies that are distinct from those of the known OCs. GRO 95551 possesses RC-like (Zhu et al., 2021a) and EC-like (Mougel et al., 2018; Qin et al., 2010a; Trinquier et al., 2007; Zhu et al., 2020a) ε^{54}Cr values, while its ε^{48}Ca value resembles those of the OCs. Its Δ^{17}O value does not match any known chondrite groups, so this chondrite likely represents a new NC chondrite parent body.

There are many ungrouped chondrites among the CCs. MIL 090292 was originally classified as a CR1 (Schrader et al., 2014). Then, it has been suggested to be an ungrouped type 1 CC because of its distinct mineralogy from GRO 95577 (CR1) and the O isotopic composition of its magnetite (Jilly-Rehak et al., 2018). Its ε^{54}Cr (1.26 ± 0.04) and Δ^{17}O (−2.21 ± 0.77 ‰) values supports it is a CR-like chondrite.

MAC 87300 and MAC 87301 are potentially paired due to their similar chondrule textures and mineralogies (Grossman, 1994), which is consistent with their similar Δ^{17}O, ε^{53}Cr, ε^{54}Cr and ε^{48}Ca values. However, they have different ε^{50}Ti values (Torrano et al., 2021), making their relationship debatable. MAC 88107 has similar a ε^{54}Cr value to those of MAC 87300 and MAC 87301, but different Δ^{17}O, ε^{50}Ti and ε^{48}Ca values, suggesting that MAC 88107 originated from another parent body. Similar to the arguments in Torrano et al. (2021), MAC 87300 and MAC 87301 may be classified as CO-like, due to their similar Δ^{17}O, ε^{50}Ti and ε^{54}Cr values as COs.

QUE 99038 is composed of many large and igneously rimmed chondrules, many CAIs and other refractory inclusions, and only a small amount of matrix. Its petrology is closer to that of a CV rather than CM (Grossman and Zipfel, 2001). Since CVs and CMs have similar ε^{54}Cr values (Zhu et al., 2021b) and the ε^{48}Ca composition for the CVs is not well constrained [from ~1.92 to ~3.92; TIMS data; (Dauphas et al., 2014; Huang and Jacobsen, 2017)], the isotope compositions reported here cannot distinguish between the two chondrite groups. Previously, Bells was regarded as a CM with unusual petrologic characteristics (Metzler et al., 1992; Mittlefehldt, 2002). Although its ε^{54}Cr value falls in the range of CMs (van Kooten et al., 2020), its distinct ε^{48}Ca value does not support Bells being a CM.

DaG 429 and DaG 430 were found close to one another (Grossman, 1999), and they have highly consistent ε^{53}Cr, ε^{54}Cr and ε^{48}Ca values, suggesting that they are paired meteorites, and are potentially also paired with DaG 055 and DaG 056 (Grossman, 1999). Their ε^{54}Cr and Δ^{17}O values (Greenwood et al., 2020) indicate that they are CO-like or CV-like chondrites, but their ε^{48}Ca values do not overlap with that of one CO chondrite, Lancé with ε^{48}Ca = 3.87 ± 0.56 (Dauphas et al., 2014). As for DaG 978, its ε^{54}Cr value is also consistent with a CO- or CM-like grouping, but that is not the case for the ε^{48}Ca systematics. Since there is presently no precise ε^{48}Ca compositions for the CVs, it cannot be inferred that DaG 978 is a CV-like chondrite.

Previous study of NWA 1152 show that its petrographic characteristics are similar to those of CRs, while its O isotope composition is similar to CVs (Smith et al., 2004). Interestingly, its ε^{54}Cr and ε^{48}Ca values overlap with those of CVs and CRs, respectively. This chondrite's intermediate isotopic compositions suggest that it represents a distinct CC parent body. NWA 12416 is regarded as a CO-like chondrite because it possesses small chondrules and CO-like bulk Δ^{17}O values (Gattacceca et al., 2020; Greenwood et al., 2020). However, its ε^{54}Cr (~1.4) and ε^{48}Ca (close to 0) values do not support a genetic relationship with the COs or any other CC group. Hence, NWA 12416 may represent yet another poorly sampled CC parent body.

BUC 10933, MIL 07513 and MIL 090001 were originally classified as CR2s (Garvie, 2012; Ruzicka et al., 2015). However, for BUC 10933 and MIL 07513 neither their ε^{54}Cr nor their ε^{48}Ca values match those of CRs. Hence, they are better regarded as ungrouped C2s. The classification for MIL 090001 has been debated between a CV or CR chondrite. It has similar ε^{48}Ca compositions to CR chondrites is consistent with a CR classification. However, MIL 090001 has a different N isotope composition from other CRs (Alexander et al., 2013).

Ningqiang is a unique ungrouped C3 chondrite. Detailed petrological, mineralogical, O isotopic and bulk chemical studies indicate that it bears many similarities with oxidized CV and CK group chondrites (Kallemeyn et al., 1991; Rubin et al., 1988; Wang and Hsu, 2009). For instance, its chondrule and matrix abundances are CV-like, while refractory lithophile elements (1.01 × CI on average) are closer to the CK (1.20 × CI) than CV (1.29 × CI) groups (Wang and Hsu, 2009). Thus, its classification has been controversial. Zhu et al. (2021b) has found a clear ε^{54}Cr difference between bulk CK (0.51 ± 0.15, 2SD) and CV (0.89 ± 0.30, 2SD) chondrites. Therefore, the ε^{54}Cr value (0.75 ± 0.08) suggests that Ningqiang is more like a CV chondrite.

4.3. Revisiting the ^{26}Al-^{26}Mg and ^{53}Mn-^{53}Cr chronology of chondrites

In this study, we report high-precision ^{26}Al-^{26}Mg data for one EH chondrite, one K chondrite and a number of ungrouped CCs and NCs. Fig. 3 combines our data with high-precision ^{26}Al-^{26}Mg data for individual meteorites taken from the literature (Larsen et al., 2011; Luu et al., 2019; van Kooten et al., 2020; Van Kooten et al., 2016). As can be seen, there is no well-defined ^{26}Al-^{26}Mg correlation line for all the chondrites, with MSWD = 21. However, we can still calculate the corresponding ^{26}Al/^{27}Al ratio of (2.27 ± 0.69) × 10^{-5}, anchored to CAIs with ^{26}Al/^{27}Al ratio of (5.23 ± 0.13) × 10^{-5} (Jacobsen et al., 2008) and absolute age of 4567.3 ± 0.13 Ma (Connelly et al., 2012). In Fig. 3b, we show the ^{26}Al-^{26}Mg chondrite group averages, and there

is still a lack of a relationship between $^{27}Al/^{24}Mg$ ratios and $\mu^{26}Mg^*$ values. Although all the ungrouped chondrites in this study are finds, given that there are no systematic differences of Al/Mg ratios between of OC and EC falls and finds (e.g., Kramer Creek, Barratta, SAH 97096 and SAH 97159 are finds), the influence of terrestrial weathering on their Al/Mg ratios should be minor. This poor correlation in Fig. 3 is caused by the CR chondrites (Luu et al., 2019), the K chondrite, and some ungrouped chondrites with $^{27}Al/^{24}Mg$ ratios of ~0.13 and ~0.19. Two ungrouped NC chondrites (with few CAIs), MIL 15362 and GRO 95551, have high $^{27}Al/^{24}Mg$ ratios, but low $\mu^{26}Mg^*$. This could be caused by their late formation time, or low initial $\mu^{26}Mg^*$ values that suggests a heterogeneous distribution of ^{26}Al in the solar system (Larsen et al., 2011). The lack of an Al-Mg correlation persists if only considering the CCs. Therefore, the Al/Mg and $\mu^{26}Mg^*$ variations cannot solely be explained as a mixing of two end-members originating from a common reservoir, e.g., CAIs and other silicates (Luu et al., 2019).

There is no *a priori* reason why all the chondrites should form a common ^{26}Al-^{26}Mg isochron since they have distinct photochemical and/or nucleosynthetic isotope anomalies, including O, Cr, Ti, Ni, Ca, Mo (Budde et al., 2019; Clayton and Mayeda, 1999; Dauphas et al., 2014; Qin et al., 2010a; Schiller et al., 2018; Steele et al., 2012; Trinquier et al., 2007; Trinquier et al., 2009; Zhang et al., 2012; Zhu et al., 2021b), reflecting variability in the makeup of their precursors and/or their formation environments within the protoplanetary disk. Rather, chondrites are complex assemblages of CAIs, AOAs, chondrules and matrix (Alexande, 2019a) that formed at different times and under varying conditions (Connelly et al., 2012). For example, although CAIs and some chondrules did form at the same time (see the internal isochron ages; Connelly et al., 2012; Bollard et al., 2017), these objects have distinct nucleosynthetic anomalies [Cr and Ti: (Gerber et al., 2017; Trinquier et al., 2009; Zhu et al., 2019a; Zhu et al., 2020a)], and, as such, must have formed in distinct reservoirs. The matrix also has a distinct origin based on its variable nucleosynthetic isotope signatures [Cr, Ti, Mo and W; (Budde et al., 2016a; Budde et al., 2016b; Schneider et al., 2020)]. The implications of a similar lack of a bulk correlation in the ^{53}Mn-^{53}Cr systematics in chondrites, and has been discussed by Zhu et al. (2021b) and Zhu et al. (2021a). Thus, chondrites are mixed assemblages of different components with different formation times and origins, which violates the basic rules for producing isochrons.

MIL 07513 possesses the highest $^{27}Al/^{24}Mg$ ratio and $\mu^{26}Mg^*$ value among all the chondrites analyzed to date, which may be related to it also having the highest $\varepsilon^{48}Ca$ value. CAIs usually have much higher $^{27}Al/^{24}Mg$ ratios (up to ~8), $\mu^{26}Mg^*$ (up to ~3000 μ) and $\varepsilon^{48}Ca$ values (up to ~6) than bulk chondrites (Bouvier and Wadhwa, 2010; Jacobsen et al., 2008; MacPherson et al., 2010; Moynier et al., 2010; Schiller et al., 2015b; Thrane et al., 2006). Given that CAIs are rich in Ca and Al, if present in significant abundance they will influence the bulk Al/Mg ratios and Ca isotope compositions of chondrites. The CVs, for instance, have high CAI contents (Krot et al., 2014) and also exhibit higher Al/Mg ratios and $\varepsilon^{48}Ca$ values than most other chondrites. Amoeboid olivine aggregates (AOAs) also have elevated $\mu^{26}Mg^*$ values, ranging from ~16 ppm to ~120 ppm (Larsen et al., 2011), and can also potentially have a large effect on the bulk $\mu^{26}Mg^*$ composition of a chondrite. This is especially true for the CVs, COs and CMs that have high AOA contents (Krot et al., 2014). However, their $^{27}Al/^{24}Mg$ ratios are not particularly high (0.08 – 0.36; Larsen et al., 2011), so that they may not modify the $^{27}Al/^{24}Mg$ ratios of bulk chondrites greatly. Chondrules and matrix account for >90 vol% of most chondrites and can also contribute to the variations in $^{27}Al/^{24}Mg$ ratios, and $\mu^{26}Mg^*$ and $\varepsilon^{48}Ca$ values of bulk chondrites. CR chondrules have $^{27}Al/^{24}Mg$ ratios that are similar to bulk CVs and CRs, while CV and CM chondrules have systematically lower $^{27}Al/^{24}Mg$ ratios than bulk CMs (Olsen et al., 2016; van Kooten et al., 2020). This could be the result of high contents of CAIs in CV and CM chondrule precursors (Krot et al., 2014). Moreover, CV chondrules have similar $\mu^{26}Mg^*$ values but higher $^{27}Al/^{24}Mg$ ratios than CM chondrules (Olsen et al., 2016; van Kooten et al., 2020). CV chondrules also have similar $^{27}Al/^{24}Mg$ ratios but higher $\mu^{26}Mg^*$ values than CR chondrules (Olsen et al., 2016). As for $\varepsilon^{48}Ca$ systematics, one OC has chondrules with heterogeneous but NC-like (i.e., < 0) $\varepsilon^{48}Ca$ values, while two CR chondrules show homogeneous $\varepsilon^{48}Ca$ values similar to those of bulk CR chondrites (Schiller et al., 2018). These $^{27}Al/^{24}Mg$, $\mu^{26}Mg^*$ and $\varepsilon^{48}Ca$ differences between chondrules from different chondrite groups, resulting from their different formation times and precursor compositions, also contribute to the lack of an Al-Mg correlation amongst bulk chondrites. Overall, there is no well-defined ^{26}Al-^{26}Mg correlation amongst bulk chondrites, and the positive trend between $^{27}Al/^{24}Mg$ and $\mu^{26}Mg^*$ mostly reflect a rough mixing of high and low Al/Mg ratio reservoirs.

Fig. 4 shows the bulk Mn-Cr systematics in chondrites. Tagish Lake (C2) is highly altered and very rich in carbonates that possess high Mn/Cr ratios (Zolensky et al., 2002). As a result, the measured Mn-Cr data may not represent its primitive composition (Petitat et al., 2011), and it is not included in the figure. In addition to the data reported in literature (Göpel et al., 2015; Qin et al., 2010a; Trinquier et al., 2008b; Zhu et al., 2021a; Zhu et al., 2021b), we have added one K chondrite and more ungrouped chondrites. It can be seen that LEW 87232 [K] shows the highest $^{55}Mn/^{52}Cr$ ratio and $\varepsilon^{53}Cr$ value, leading to a positive trend between $^{55}Mn/^{52}Cr$ ratios and $\varepsilon^{53}Cr$ values among all the chondrites. As for the Al-Mg system, there is also no well-defined Mn-Cr correlation line, and this can also be caused by the different origins of the chondrites and/or multiple chondritic components mixing, as discussed in Zhu et al. (2021a) and Zhu et al. (2021b) in detail.

5. Conclusion

This study reports high-precision mass-independent Cr, Ca and Mg isotope data for enstatite meteorites, Kakangari and ungrouped chondrites. The results are used to discuss the diversity of chondrite isotope reservoirs, test the CC-NC dichotomy, explore the potential classification of the ungrouped chondrites, and revisit the bulk ^{53}Mn-^{53}Cr and ^{26}Al-^{26}Mg chronology of chondrites. This large dataset is used to reach the following conclusions:

1. One primitive EH3 enstatite chondrite (SAH 97096) has a $\varepsilon^{48}Ca$ value of −0.19 ± 0.22, which is similar to the Ca isotope composition of the Earth, Moon and maybe the ordinary chondrites.
2. Itqiy [EH7] and two other potentially related enstatite-rich rocks from the Almahatta Sitta fall show similar $\varepsilon^{48}Ca$ compositions, −0.35 ± 0.10 (2SD), which is different from those of the Earth-Moon system. This suggests the existence of a distinct Itqiy parent body, consistent with their $\varepsilon^{54}Cr$ values.
3. The first nucleosynthetic isotope data for one Kakangari chondrite, LEW 87232, is reported with $\varepsilon^{48}Ca$ and $\varepsilon^{54}Cr$ values of-1 .30 ± 0.25 and −0.44 ± 0.04 respectively, indicating that it belongs to the NCs.
4. All the ungrouped carbonaceous chondrites show positive $\varepsilon^{54}Cr$ and $\varepsilon^{48}Ca$ values, and all the ungrouped non-carbonaceous chondrites show zero or negative $\varepsilon^{54}Cr$ and $\varepsilon^{48}Ca$ values. This observation confirms the CC-NC dichotomy for the solar system materials.
5. Based on the new $\varepsilon^{54}Cr$ and $\varepsilon^{48}Ca$ values, as well as their previously determined isotopic and petrologic properties, none the ungrouped chondrites belong to any of the known chondrite groups, and they probably come from separate chondrite parent bodies.

6. When the ungrouped chondrite data are combined with the literature data for chondrites, there are no well-defined bulk ^{26}Al-^{26}Mg and ^{53}Mn-^{53}Cr correlation lines. Hence, the bulk chondrite compositions cannot be explained by mixing of only two endmembers (e.g., CAIs and other silicates), but are the result of multiple-component mixing.

Declaration of Competing Interest

The authors declare that they have no known competing financial interests or personal relationships that could have appeared to influence the work reported in this paper.

Acknowledgements

K. Z. thanks Alexander von Humboldt postdoc fellowship, China Scholarship Council (CSC) PhD fellowship (#201706340161), and a UK STFC grant (#ST/V000888/1). F. M. acknowledges funding from the European Research Council under the H2020 framework program/ERC Starting Grant Agreement (#637503–PRISTINE) and financial support of the UnivEarthS Labex program at Sorbonne Paris Cité (#ANR–10–LABX–0023 and #ANR–11–IDEX-0005-02), and the ANR through a chaire d'excellence Sorbonne Paris Cité. M. B. acknowledges funding the Carlsberg Foundation (CF18-1105), the Danish National Research Foundation (DNRF97) and the European Research Council (ERC Advanced Grant Agreement, #833275–DEEPTIME). M. S. acknowledges funding from the Villum Fonden (#00025333). Pierre Burckel is acknowledged for ICP-MS analysis, and Matt Jackson is acknowledged for providing the two terrestrial peridotites. Parts of this work were supported by IPGP multidisciplinary program PARI, and by Paris–IdF region SESAME (#12015908). US Antarctic meteorite samples are recovered by the Antarctic search for Meteorites (ANSMET) program which has been funded by NSF and NASA, and characterized and curated in the Department of Mineral Sciences of the Smithsonian Institution and Astromaterials Curation Office at NASA Johnson Space Center. Yun Jiang is appreciated for providing Ningqiang meteorite. Comments from Stefan Weyer (AE) and three anonymous reviewers improved this manuscript.

Appendix A. Supplementary material

Supplementary material (1. data sources and 2. ε^{46}Ca data) to this article can be found online at https://doi.org/10.1016/j.gca.2022.12.014.

References

Alexander, C.M.O.D., Howard, K.T., Bowden, R., Fogel, M.L., 2013. The classification of CM and CR chondrites using bulk H, C and N abundances and isotopic compositions. Geochim. Cosmochim. Acta 123, 244–260.
Alexander, C.M.O.D., 2019a. Quantitative models for the elemental and isotopic fractionations in chondrites: The carbonaceous chondrites. Geochim. Cosmochim. Acta 254, 277–309.
Alexander, C.M.O.D., 2019b. Quantitative models for the elemental and isotopic fractionations in the non-carbonaceous chondrites. Geochim. Cosmochim. Acta 254, 246–276.
Allègre, C.J., Poirier, J.-P., Humler, E., Hofmann, A.W., 1995. The chemical composition of the Earth. Earth Planet. Sci. Lett. 134, 515–526.
Bischoff, A., Alexander, C.M.O.D., Barrat, J.-A., Burkhardt, C., Busemann, H., Degering, D., Di Rocco, T., Fischer, M., Fockenberg, T., Foustoukos, D.I., Gattacceca, J., Godinho, J.R.A., Harries, D., Heinlein, D., Hellmann, J.L., Hertkorn, N., Holm, A., Jull, A.J.T., Kerraouch, I., King, A.J., Kleine, T., Koll, D., Lachner, J., Ludwig, T., Merchel, S., Mertens, C.A.K., Morino, P., Neumann, W., Pack, A., Patzek, M., Pavetich, S., Reitze, M.P., Rüfenacht, M., Rugel, G., Schmidt, C., Schmitt-Kopplin, P., Schönbächler, M., Trieloff, M., Wallner, A., Wimmer, K., Wölfer, E., 2021. The old, unique C1 chondrite Flensburg – Insight into the first processes of aqueous alteration, brecciation, and the diversity of water-bearing parent bodies and lithologies. Geochim. Cosmochim. Acta 293, 142–186.
Bischoff, A., Bannemann, L., Decker, S., Ebert, S., Haberer, S., Heitmann, U., Horstmann, M., Klemm, K.I., Kraemer, A.-K., Lentfort, S., Patzek, M., Storz, J., Weyrauch, M., 2022. Asteroid 2008 TC3, not a polymict ureilitic but a polymict C1 chondrite parent body? Survey of 249 Almahata Sitta fragments. Meteorit. Planet. Sci. 57, 1339–1364.
Bizzarro, M., Paton, C., Larsen, K., Schiller, M., Trinquier, A., Ulfbeck, D., 2011. High-precision Mg-isotope measurements of terrestrial and extraterrestrial material by HR-MC-ICPMS—implications for the relative and absolute Mg-isotope composition of the bulk silicate Earth. J. Anal. At. Spectrom 26, 565–577.
Bollard, J., Connelly, J.N., Whitehouse, J.J., Pringle, E.A., Bonal, L., Jørgensen, J.K., Nordlund, Åke, Moynier, F., Bizzarro, M., 2017. Early formation of planetary building blocks inferred from Pb isotopic ages of chondrules. Science Advances 3, (8) e1700407.
Bouvier, A., Wadhwa, M., 2010. The age of the Solar System redefined by the oldest Pb–Pb age of a meteoritic inclusion. Nat. Geosci. 3, 637–641.
Brasser, R., Mojzsis, S.J., 2020. The partitioning of the inner and outer Solar System by a structured protoplanetary disk. Nat. Astron 4, 492–499.
Budde, G., Burkhardt, C., Brennecka, G.A., Fischer-Gödde, M., Kruijer, T.S., Kleine, T., 2016a. Molybdenum isotopic evidence for the origin of chondrules and a distinct genetic heritage of carbonaceous and non-carbonaceous meteorites. Earth Planet. Sci. Lett. 454, 293–303.
Budde, G., Kleine, T., Kruijer, T.S., Burkhardt, C., Metzler, K., 2016b. Tungsten isotopic constraints on the age and origin of chondrules. Proc. Nat. Acad. Sci. 113, 201524980.
Budde, G., Burkhardt, C., Kleine, T., 2019. Molybdenum isotopic evidence for the late accretion of outer Solar System material to Earth. Nature Astron. 1.
Chen, H.-W., Lee, T., Lee, D.-C., Jiun-San Shen, J., Chen, J.-C., 2011. ^{48}Ca heterogeneity in differentiated meteorites. Astrophys. J. Lett. 743, L23.
Clayton, R.N., Mayeda, T.K., 1984. The oxygen isotope record in Murchison and other carbonaceous chondrites. Earth Planet. Sci. Lett. 67, 151–161.
Clayton, R.N., Mayeda, T.K., 1988. Formation of ureilites by nebular processes. Geochim. Cosmochim. Acta 52, 1313–1318.
Clayton, R.N., Mayeda, T.K., 1999. Oxygen isotope studies of carbonaceous chondrites. Geochim. Cosmochim. Acta 63, 2089–2104.
Clayton, R.N., Mayeda, T.K., Rubin, A.E., 1984. Oxygen isotopic compositions of enstatite chondrites and aubrites. J. Geophys. Res. Solid Earth 89, C245–C249.
Clayton, R.N., Mayeda, T.K., Goswami, J., Olsen, E.J., 1991. Oxygen isotope studies of ordinary chondrites. Geochim. Cosmochim. Acta 55, 2317–2337.
Cohen, B.A., Goodrich, C.A., Keil, K., 2004. Feldspathic clast populations in polymict ureilites: Stalking the missing basalts from the ureilite parent body. Geochim. Cosmochim. Acta 68, 4249–4266.
Connelly, J.N., Bizzarro, M., Krot, A.N., Nordlund, Å., Wielandt, D., Ivanova, M.A., 2012. The absolute chronology and thermal processing of solids in the solar protoplanetary disk. Science 338, 651–655.
Dauphas, N., Chen, J.H., Zhang, J., Papanastassiou, D.A., Davis, A.M., Travaglio, C., 2014. Calcium-48 isotopic anomalies in bulk chondrites and achondrites: evidence for a uniform isotopic reservoir in the inner protoplanetary disk. Earth Planet. Sci. Lett. 407, 96–108.
Davis, A.M., Grossman, L., Ganapathy, R., 1977. Yes, Kakangari is a unique chondrite. Nature 265, 230–232.
Garvie, L.A.J., 2012. The Meteoritical Bulletin, No. 99. Meteorit. Planet. Sci. 47, E1–E52.
Gattacceca, J., McCubbin, F.M., Bouvier, A., Grossman, J.N., 2020. The Meteoritical Bulletin, no. 108. Meteorit. Planet. Sci. 55, 1146–1150.
Gattacceca, J., McCubbin, F.M., Grossman, J., Bouvier, A., Bullock, E., Chennaoui Aoudjehane, H., Debaille, V., D'Orazio, M., Komatsu, M., Miao, B., Schrader, D. L., 2021. The Meteoritical Bulletin, No. 109. Meteorit. Planet. Sci. 56, 1626–1630.
Gerber, S., Burkhardt, C., Budde, G., Metzler, K., Kleine, T., 2017. Mixing and Transport of Dust in the Early Solar Nebula as Inferred from Titanium Isotope Variations among Chondrules. The Astrophysical Journal Letters 841, L17.
Goodrich, C.A., Hartmann, W.K., O'Brien, D.P., Weidenschilling, S.J., Wilson, L., Michel, P., Jutzi, M., 2015. Origin and history of ureilitic material in the solar system: The view from asteroid 2008 TC 3 and the Almahata Sitta meteorite. Meteorit. Planet. Sci. 50, 782–809.
Goodrich, C.A., 1992. Ureilites: A critical review. Meteoritics 27, 327–352.
Greenwood, R.C., Burbine, T.H., Miller, M.F., Franchi, I.A., 2017. Melting and differentiation of early-formed asteroids: The perspective from high precision oxygen isotope studies. Chem. Erde 77, 1–43.
Greenwood, R.C., Burbine, T.H., Franchi, I.A., 2020. Linking asteroids and meteorites to the primordial planetesimal population. Geochim. Cosmochim. Acta 277, 377–406.
Grossman, J.N., Zipfel, J., 2001. The meteoritical bulletin, no. 85, 2001 september. Meteorit. Planet. Sci. 36, A293–A322.
Grossman, J.N., 1994. The meteoritical bulletin, no. 76, 1994 January: The US Antarctic meteorite collection. Meteoritics 29, 100–143.
Grossman, J.N., 1999. The meteoritical bulletin, no. 83, 1999 July. Meteorit. Planet. Sci. 34, A169–A186.
Göpel, C., Birck, J.-L., Galy, A., Barrat, J.-A., Zanda, B., 2015. Mn–Cr systematics in primitive meteorites: Insights from mineral separation and partial dissolution. Geochim. Cosmochim. Acta 156, 1–24.
Harries, D., Bischoff, A., 2020. Petrological evidence for the existence and disruption of a 500 km-sized differentiated planetesimal of enstatite-chondritic parentage. Earth Planet. Sci. Lett. 548, 116506.
Hauri, E.H., Shimizu, N., Dieu, J.J., Hart, S.R., 1993. Evidence for hotspot-related carbonatite metasomatism in the oceanic upper mantle. Nature 365, 221–227.

Horstmann, M., Bischoff, A., 2014. The Almahata Sitta polymict breccia and the late accretion of asteroid 2008 TC3. Geochemistry 74, 149–183.
Huang, S., Jacobsen, S.B., 2017. Calcium isotopic compositions of chondrites. Geochim. Cosmochim. Acta 201, 364–376.
Inglis, E.C., Creech, J.B., Deng, Z., Moynier, F., 2018. High-precision zirconium stable isotope measurements of geological reference materials as measured by double-spike MC-ICPMS. Chem. Geol. 493, 544–552.
Jacobsen, B., Yin, Q.-Z., Moynier, F., Amelin, Y., Krot, A.N., Nagashima, K., Hutcheon, I. D., Palme, H., 2008. 26 Al–26 Mg and 207 Pb–206 Pb systematics of Allende CAIs: Canonical solar initial 26 Al/27 Al ratio reinstated. Earth Planet. Sci. Lett. 272, 353–364.
Javoy, M., Kaminski, E., Guyot, F., Andrault, D., Sanloup, C., Moreira, M., Labrosse, S., Jambon, A., Agrinier, P., Davaille, A., 2010. The chemical composition of the Earth: Enstatite chondrite models. Earth Planet. Sci. Lett. 293, 259–268.
Javoy, M., 1995. The integral enstatite chondrite model of the Earth. Geophys. Res. Lett. 22, 2219–2222.
Jilly-Rehak, C.E., Huss, G.R., Nagashima, K., Schrader, D.L., 2018. Low-temperature aqueous alteration on the CR chondrite parent body: Implications from in situ oxygen-isotope analyses. Geochim. Cosmochim. Acta 222, 230–252.
Kallemeyn, G.W., Rubin, A.E., Wasson, J.T., 1991. The compositional classification of chondrites: V. The Karoonda (CK) group of carbonaceous chondrites. Geochim. Cosmochim. Acta 55, 881–892.
Keil, K., Bischoff, A., 2008. Northwest Africa 2526: A partial melt residue of enstatite chondrite parentage. Meteorit. Planet. Sci. 43, 1233–1240.
Kleine, T., Budde, G., Burkhardt, C., Kruijer, T.S., Worsham, E.A., Morbidelli, A., Nimmo, F., 2020. The non-carbonaceous–carbonaceous meteorite dichotomy. Space Sci. Rev. 216, 1–27.
Krot, A.N., Keil, K., Scott, E.R.D., Goodrich, C.A., Weisberg, M.K., 2014. 1.1 - Classification of Meteorites and Their Genetic Relationships A2 - Holland, Heinrich D. In: Turekian, K.K. (Ed.), Treatise on Geochemistry. Second ed.,. Elsevier, Oxford, pp. 1–63.
Kruijer, T.S., Burkhardt, C., Budde, G., Kleine, T., 2017. Age of Jupiter inferred from the distinct genetics and formation times of meteorites. Proc. Natl. Acad. Sci. 114, 6712–6716.
Larsen, K.K., Trinquier, A., Paton, C., Schiller, M., Wielandt, D., Ivanova, M.A., Connelly, J.N., Nordlund, Å., Krot, A.N., Bizzarro, M., 2011. Evidence for magnesium isotope heterogeneity in the solar protoplanetary disk. Astrophys. J. Lett. 735, L37.
Larsen, K.K., Schiller, M., Bizzarro, M., 2016a. Accretion timescales and style of asteroidal differentiation in an ^{26}Al-poor protoplanetary disk. Geochim. Cosmochim. Acta 176, 295–315.
Larsen, K.K., Wielandt, D., Schiller, M., Bizzarro, M., 2016b. Chromatographic speciation of Cr(III)-species, inter-species equilibrium isotope fractionation and improved chemical purification strategies for high-precision isotope analysis. J. Chromatogr. A 1443, 162–174.
Larsen, K.K., Wielandt, D., Bizzarro, M., 2018. Multi-element ion-exchange chromatography and high-precision MC-ICP-MS isotope analysis of Mg and Ti from sub-mm-sized meteorite inclusions. J. Anal. At. Spectrom 33, 613–628.
Lewis, J., Luu, T.-H., Coath, C.D., Wehrs, H., Schwieters, J.B., Elliott, T., 2022. Collision course; high-precision mass-independent and mass-dependent calcium isotope measurements using the prototype collision cell MC-ICPMS/MS. Proteus. Chem. Geol. 614, 121185.
Leya, I., Schönbächler, M., Wiechert, U., Krähenbühl, U., Halliday, A.N., 2008. Titanium isotopes and the radial heterogeneity of the solar system. Earth Planet. Sci. Lett. 266, 233–244.
Lichtenberg, T., Drażkowska, J., Schönbächler, M., Golabek, G.J., Hands, T.O., 2021. Bifurcation of planetary building blocks during Solar System formation. Science 371, 365–370.
Lugmair, G., Shukolyukov, A., 1998. Early solar system timescales according to 53 Mn-53 Cr systematics. Geochim. Cosmochim. Acta 62, 2863–2886.
Luu, T.-H., Hin, R.C., Coath, C.D., Elliott, T., 2019. Bulk chondrite variability in mass independent magnesium isotope compositions – Implications for initial solar system ^{26}Al/^{27}Al and the timing of terrestrial accretion. Earth Planet. Sci. Lett. 522, 166–175.
MacPherson, G.J., Bullock, E.S., Janney, P.E., Kita, N.T., Ushikubo, T., Davis, A.M., Wadhwa, M., Krot, A.N., 2010. Early solar nebula condensates with canonical, not supracanonical, initial ^{26}Al/^{27}Al ratios. Astrophys. J. 711, L117–L121.
Mason, B., 1963. The carbonaceous chondrites. Space Sci. Rev. 1, 621–646.
McDonough, W.F., Sun, S.-S., 1995. The composition of the Earth. Chem. Geol. 120, 223–253.
Metzler, K., Bischoff, A., Stöffler, D., 1992. Accretionary dust mantles in CM chondrites: Evidence for solar nebula processes. Geochim. Cosmochim. Acta 56, 2873–2897.
Mittlefehldt, D.W., 2002. Geochemistry of the ungrouped carbonaceous chondrite Tagish Lake, the anomalous CM chondrite Bells, and comparison with CI and CM chondrites. Meteorit. Planet. Sci. 37, 703–712.
Mostefaoui, S., Perron, C., Zinner, E., Sagon, G., 2000. Metal-associated carbon in primitive chondrites: structure, isotopic composition, and origin. Geochim. Cosmochim. Acta 64, 1945–1964.
Mougel, B., Moynier, F., Göpel, C., 2018. Chromium isotopic homogeneity between the Moon, the Earth, and enstatite chondrites. Earth Planet. Sci. Lett. 481, 1–8.
Moynier, F., Fegley Jr, B., 2015. The Earth's building blocks. Early Earth: Accret. Different., 27–47
Moynier, F., Justin, I.S., Frank, A.P., Bradley, S.M., Joyce, B., Donald, J.D., 2010. Ca Isotope effects in orgueil leachates and the implications for the carrier phases of ^{54}Cr anomalies. Astrophys. J. Lett. 718, L7.
Moynier, F., Deng, Z., Lanteri, A., Martins, R., Chaussidon, M., Savage, P., Siebert, J., 2020. Metal-silicate silicon isotopic fractionation and the composition of the bulk Earth. Earth Planet. Sci. Lett. 549, 116468.
Olsen, M.B., Wielandt, D., Schiller, M., Van Kooten, E.M.M.E., Bizzarro, M., 2016. Magnesium and ^{54}Cr isotope compositions of carbonaceous chondrite chondrules – Insights into early disk processes. Geochim. Cosmochim. Acta 191, 118–138.
Otting, W., Zähringer, J., 1967. Total carbon content and primordial rare gases in chondrites. Geochim. Cosmochim. Acta 31, 1949–1960.
Palme, H., O'Neill, H.S.C., 2014. 3.1 - Cosmochemical estimates of mantle composition. In: Holland, H.D., Turekian, K.K. (Eds.), Treatise on Geochemistry. second ed. Elsevier, Oxford, pp. 1–39.
Patzer, A., Hill, D.H., Boynton, W.V., 2001. Itqiy: A metal-rich enstatite meteorite with achondritic texture. Meteorit. Planet. Sci. 36, 1495–1505.
Pedersen, S.G., Schiller, M., Connelly, J.N., Bizzarro, M., 2019. Testing accretion mechanisms of the H chondrite parent body utilizing nucleosynthetic anomalies. Meteorit. Planet. Sci. 54, 1215–1227.
Petitat, M., Birck, J.-L., Luu, T., Gounelle, M., 2011. The chromium isotopic composition of the ungrouped carbonaceous chondrite Tagish Lake. Astrophys J 736, 23.
Qin, L., Alexander, C.M.O.D., Carlson, R.W., Horan, M.F., Yokoyama, T., 2010a. Contributors to chromium isotope variation of meteorites. Geochim. Cosmochim. Acta 74, 1122–1145.
Qin, L., Rumble, D., Alexander, C.M.O.D., Carlson, R.W., Jenniskens, P., Shaddad, M.H., 2010b. The chromium isotopic composition of Almahata Sitta. Meteorit. Planet. Sci. 45, 1771–1777.
Quitté, G., Markowski, A., Latkoczy, C., Gabriel, A., Pack, A., 2010. Iron-60 heterogeneity and incomplete isotope mixing in the early solar system. Astrophys J 720, 1215.
Rubin, A.E., Wang, D., Kallemeyn, G.W., Wasson, J.T., 1988. The Ningqiang meteorite: Classification and petrology of an anomalous CV chondrite. Meteoritics 23, 13–23.
Ruzicka, A., Grossman, J., Bouvier, A., Herd, C.D.K., Agee, C.B., 2015. The meteoritical bulletin, No. 102. Wiley Online Library.
Sanborn, M.E., Wimpenny, J., Williams, C.D., Yamakawa, A., Amelin, Y., Irving, A.J., Yin, Q.-Z., 2019. Carbonaceous Achondrites Northwest Africa 6704/6693: Milestones for early solar system chronology and genealogy. Geochim. Cosmochim. Acta 245, 577–596.
Schiller, M., Connelly, J.N., Glad, A.C., Mikouchi, T., Bizzarro, M., 2015a. Early accretion of protoplanets inferred from a reduced inner solar system ^{26}Al inventory. Earth Planet. Sci. Lett. 420, 45–54.
Schiller, M., Paton, C., Bizzarro, M., 2015b. Evidence for nucleosynthetic enrichment of the protosolar molecular cloud core by multiple supernova events. Geochim. Cosmochim. Acta 149, 88–102.
Schiller, M., Bizzarro, M., Fernandes, V.A., 2018. Isotopic evolution of the protoplanetary disk and the building blocks of Earth and the Moon. Nature 555, 507.
Schiller, M., Bizzarro, M., Siebert, J., 2020. Iron isotope evidence for very rapid accretion and differentiation of the proto-Earth. Sci. Adv. 6, eaay7604.
Schneider, J.M., Burkhardt, C., Marrocchi, Y., Brennecka, G.A., Kleine, T., 2020. Early evolution of the solar accretion disk inferred from Cr-Ti-O isotopes in individual chondrules. Earth Planet. Sci. Lett. 551, 116585.
Schrader, D.L., Davidson, J., Greenwood, R.C., Franchi, I.A., Gibson, J.M., 2014. A water–ice rich minor body from the early Solar System: The CR chondrite parent asteroid. Earth Planet. Sci. Lett. 407, 48–60.
Shuai, K., Hui, H., Zhou, L., Li, W., 2022. Accretion regions of meteorite parent bodies inferred from a two-endmember isotopic mixing model. MNRAS stac849.
Shukolyukov, A., Lugmair, G., 2006. Manganese–chromium isotope systematics of carbonaceous chondrites. Earth Planet. Sci. Lett. 250, 200–213.
Smith, C.L., Russell, S.S., Gounelle, M., Greenwood, R.C., Franchi, I.A., 2004. NWA 1152 and Sahara 00182: New primitive carbonaceous chondrites with affinities to the CR and CV groups. Meteorit. Planet. Sci. 39, 2009–2032.
Steele, R.C.J., Coath, C.D., Regelous, M., Russell, S., Elliott, T., 2012. Neutron-poor nickel isotope anomalies in meteorites. Astrophys. J. 758, 59.
Thrane, K., Bizzarro, M., Baker, J.A., 2006. Extremely brief formation interval for refractory inclusions and uniform distribution of ^{26}Al in the early solar system. Astrophys. J. Lett. 646, L159.
Torrano, Z.A., Schrader, D.L., Davidson, J., Greenwood, R.C., Dunlap, D.R., Wadhwa, M., 2021. The relationship between CM and CO chondrites: Insights from combined analyses of titanium, chromium, and oxygen isotopes in CM, CO, and ungrouped chondrites. Geochim. Cosmochim. Acta 301, 70–90.
Trinquier, A., Birck, J.-L., Allègre, C.J., 2007. Widespread ^{54}Cr heterogeneity in the inner solar system. Astrophys J 655, 1179–1185.
Trinquier, A., Birck, J.-L., Allègre, C.J., 2008a. High-precision analysis of chromium isotopes in terrestrial and meteorite samples by thermal ionization mass spectrometry. J. Anal. At. Spectrom 23, 1565–1574.
Trinquier, A., Birck, J.L., Allègre, C.J., Göpel, C., Ulfbeck, D., 2008b. ^{53}Mn–^{53}Cr systematics of the early Solar System revisited. Geochim. Cosmochim. Acta 72, 5146–5163.
Trinquier, A., Elliott, T., Ulfbeck, D., Coath, C., Krot, A.N., Bizzarro, M., 2009. Origin of nucleosynthetic isotope heterogeneity in the solar protoplanetary disk. Science 324, 374–376.
Van Kooten, E.M.M.E., Wielandt, D., Schiller, M., Nagashima, K., Thomen, A., Larsen, K.K., Olsen, M.B., Nordlund, Å., Krot, A.N., Bizzarro, M., 2016. Isotopic evidence for primordial molecular cloud material in metal-rich carbonaceous chondrites. Proc. Natl. Acad. Sci. 113, 2011–2016.

Van Kooten, E.M.M.E., Schiller, M., Bizzarro, M., 2017. Magnesium and chromium isotope evidence for initial melting by radioactive decay of ^{26}Al and late stage impact-melting of the ureilite parent body. Geochim. Cosmochim. Acta 208, 1–23.

van Kooten, E., Cavalcante, L., Wielandt, D., Bizzarro, M., 2020. The role of Bells in the continuous accretion between the CM and CR chondrite reservoirs. Meteorit. Planet. Sci.

Vermeesch, P., 2018. IsoplotR: A free and open toolbox for geochronology. Geosci. Front. 9, 1479–1493.

Wang, Y., Hsu, W., 2009. Petrology and mineralogy of the Ningqiang carbonaceous chondrite. Meteorit. Planet. Sci. 44, 763–780.

Warren, P.H., 2011. Stable-isotopic anomalies and the accretionary assemblage of the Earth and Mars: A subordinate role for carbonaceous chondrites. Earth Planet. Sci. Lett. 311, 93–100.

Weisberg, M.K., Prinz, M., Clayton, R.N., Mayeda, T.K., Grady, M.M., Franchi, I., Pillinger, C.T., Kallemeyn, G.W., 1996. The K (Kakangari) chondrite grouplet. Geochim. Cosmochim. Acta 60, 4253–4263.

Yamaguchi, A., Clayton, R.N., Mayeda, T.K., Ebihara, M., Oura, Y., Miura, Y.N., Haramura, H., Misawa, K., Kojima, H., Nagao, K., 2002. A new source of basaltic meteorites inferred from Northwest Africa 011. Science 296, 334–336.

Yamakawa, A., Yamashita, K., Makishima, A., Nakamura, E., 2009. Chemical separation and mass spectrometry of Cr, Fe, Ni, Zn, and Cu in terrestrial and extraterrestrial materials using thermal ionization mass spectrometry. Anal. Chem. 81, 9787–9794.

Yamakawa, A., Yamashita, K., Makishima, A., Nakamura, E., 2010. Chromium isotope systematics of achondrites: Chronology and isotopic heterogeneity of the inner solar system bodies. Astrophys. J. 720, 150.

Zhang, J., Dauphas, N., Davis, A.M., Leya, I., Fedkin, A., 2012. The proto-Earth as a significant source of lunar material. Nature Geosci. 5, 251–255.

Zhu, K., Liu, J., Moynier, F., Qin, L., Alexander, C.M.O.D., He, Y., 2019a. Chromium isotopic evidence for an early formation of chondrules from the Ornans CO chondrite. Astrophys. J. 873, 82.

Zhu, K., Moynier, F., Barrat, J.-A., Wielandt, D., Larsen, K., Bizzarro, M., 2019b. Timing and origin of the angrite parent body inferred from Cr isotopes. Astrophys. J. Lett. 877, L13.

Zhu, K., Moynier, F., Schiller, M., Bizzarro, M., 2020a. Dating and tracing the origin of enstatite chondrite chondrules with Cr isotopes. Astrophys. J. Lett. 894, L26.

Zhu, K., Moynier, F., Schiller, M., Wielandt, D., Larsen, K., van Kooten, E., Bizzarro, M., 2020b. Chromium isotopic constraints on the origin the ureilite parent body. Astrophys. J. 888, 126.

Zhu, K., Moynier, F., Schiller, M., Alexander, C.M.O.D., Barrat, J.-A., Bischoff, A., Bizzarro, M., 2021a. Mass–independent and mass–dependent Cr isotopic composition of the Rumuruti (R) chondrites: Implications for their origin and planet formation. Geochim. Cosmochim. Acta 293, 598–609.

Zhu, K., Moynier, F., Schiller, M., Alexander, C.M.O.D., Davidson, J., Schrader, D.L., van Kooten, E.M.M.E., Bizzarro, M., 2021b. Chromium isotopic insights into the origin of chondrite parent bodies and the early terrestrial volatile depletion. Geochim. Cosmochim. Acta 301, 158–186.

Zhu, K., Moynier, F., Schiller, M., Barrat, J.A., Becker, H., Bizzarro, M., 2021c. Tracing the origin and core formation of the enstatite achondrite parent bodies using Cr isotopes. Geochim. Cosmochim. Acta 308, 256–272.

Zhu, K., Schiller, M., Pan, L., Saji, N.S., Larsen, K.K., Amsellem, E., Rundhaug, C., Sossi, P., Leya, I., Moynier, F., Bizzarro, M., 2022. Late delivery of exotic chromium to the crust of Mars by water-rich carbonaceous asteroids. Sci. Adv. 8, eabp8415.

Zolensky, M.E., Nakamura, K., Gounelle, M., Mikouchi, T., Kasama, T., Tachikawa, O., Tonui, E., 2002. Mineralogy of Tagish Lake: An ungrouped type 2 carbonaceous chondrite. Meteorit. Planet. Sci. 37, 737–761.